

A STUDY OF  $\text{Mg}^{24}$  LEVELS BY PROTON CAPTURE

A STUDY OF  $Mg^{24}$  LEVELS BY PROTON CAPTURE

By

KENNETH JOHN CASSELL, B.Sc.

A Thesis

Submitted to the Faculty of Graduate Studies  
in Partial Fulfilment of the Requirements  
for the Degree  
Master of Science

McMaster University

May, 1968.

MASTER OF SCIENCE (1968)  
(Physics)

McMASTER UNIVERSITY  
Hamilton, Ontario.

TITLE: A Study of  $Mg^{24}$  Levels by Proton Capture

AUTHOR: Kenneth John Cassell, B.Sc. (Borough Polytechnic,  
London, England)

SUPERVISOR: Professor J.A. Kuehner

NUMBER OF PAGES: (ix), 87.

SCOPE AND CONTENTS: The following thesis comprises the study of six resonances in the  $Na^{23}(p,\gamma)Mg^{24}$  reaction, using a 40 cu. cm. Ge(Li) detector. These resonances are at proton energies,  $E_p = 512$  Kev, 987 Kev, 1020 Kev, 1174 Kev, 1318 Kev and 1416 Kev. The decay scheme and branching ratios have been found for each of these resonances. Also the gamma transition widths have been found for all of these resonances, except the 1416 Kev resonance, and these transition widths have been employed in calculating the reduced gamma transition strengths for the above decays.

## ACKNOWLEDGEMENTS

I should like to extend my thanks to my supervisor, Professor J.A. Kuehner, for his help and understanding at all times. My thanks also to Dr. A. Baxter for his assistance in the experimental work.

I also extend my appreciation to my wife, Chris, for her typing of this thesis, and for her patience and understanding while it was being written.

## TABLE OF CONTENTS

	Page
DESCRIPTIVE NOTE	(ii)
ACKNOWLEDGEMENTS	(iii)
LIST OF FIGURES	(vi)
LIST OF TABLES	(viii)
CHAPTER 1: INTRODUCTION	1
1.1 General	1
CHAPTER 2: EXPERIMENTAL METHODS	5
2.1 Experimental Considerations	5
(i) Introduction	5
(ii) Geometry considerations	7
(iii) Electronics considerations	8
(iv) Target and backing choice	10
(v) Target and backing preparation	14
2.2 Yield curve considerations	19
2.3 Procedures for finding decay schemes	20
2.4 Procedures for finding branching ratios	23
2.5 The Ge(Li) detector relative efficiencies curve	29
2.6 Procedures for finding gamma transition widths	32

Table of Contents (continued ....)

	Page
(i) Theoretical considerations	32
(ii) Measurement of $Y(\infty)$	44
CHAPTER 3: EXPERIMENTAL RESULTS	47
3.1 Introduction	47
3.2 Results	47
(i) $E_p = 512$ Kev Resonance	47
(ii) $E_p = 987$ Kev Resonance	54
(iii) $E_p = 1020$ Kev Resonance	62
(iv) $E_p = 1174$ Kev Resonance	70
(v) $E_p = 1318$ Kev Resonance	75
(vi) $E_p = 1416$ Kev Resonance	80
3.3 Conclusion	85
BIBLIOGRAPHY	87

## LIST OF FIGURES

	Page
Figure 1: Decay Scheme for Mg <sup>24</sup>	2
Figure 2: Experimental Geometry	6
Figure 3: High Current Target	11
Figure 4: Target Evaporation Geometry	13
Figure 5: Yield Curve from NaCl Target	15
Figure 6: Yield Curve from NaOH Target	16
Figure 7: Yield Curve from 1.63 Mev Gate	17
Figure 8: Relative efficiency curve for Ge(Li)	28
Figure 9: Reactions vs. Proton Energy in a Thick Target	34
Figure 10: Theoretical Yield Curves	38
Figure 11: Atomic Stopping Cross-section for Na in NaCl	43
Figure 12: Ge(Li) Spectrum for 511 Kev Resonance	48
Figure 13: Decay Scheme for 511 Kev Resonance	51
Figure 14: Ge(Li) Spectrum for 987 Kev Resonance	55
Figure 15: Decay Scheme for 987 Kev Resonance	57
Figure 16: Ge(Li) Spectrum for 1020 Kev Resonance	60
Figure 17: Decay Scheme for 1020 Kev Resonance	63
Figure 18: Ge(Li) Spectrum for 1174 Kev Resonance	67

List of Figures (continued ....)

	Page
Figure 19: Decay Scheme for 1174 Kev Resonance	69
Figure 20: Ge(Li) Spectrum for 1318 Kev Resonance	73
Figure 21: Decay Scheme for 1318 Kev Resonance	76
Figure 22: Ge(Li) Spectrum for 1416 Kev Resonance	78
Figure 23: Decay Scheme for 1416 Kev Resonance	82

## LIST OF TABLES

	Page
Table 1: Transition Widths for $\text{Na}^{23} + p$ Resonances	3
Table 2: Identification of $\text{Na}^{23}(p,\gamma)\text{Mg}^{24}$ Resonances	18
Table 3: Identification of the Peaks in the Ge(Li) Spectrum for the 512 Kev Resonance	49
Table 4: Comparison to Single Particle Estimates in the 512 Kev Resonance	53
Table 5: Identification of the Peaks in the Ge(Li) Spectrum for the 987 Kev Resonance	56
Table 6: Comparison to Single Particle Estimates in the 987 Kev Resonance	59
Table 7: Identification of the Peaks in the Ge(Li) Spectrum for the 1020 Kev Resonance	61
Table 8: Comparison to Single Particle Estimates in the 1020 Kev Resonance	65
Table 9: Identification of the Peaks in the Ge(Li) Spectrum for the 1174 Kev Resonance	68
Table 10: Comparison to Single Particle Estimates in the 1174 Kev Resonance	72
Table 11: Identification of the Peaks in the Ge(Li) Spectrum for the 1318 Kev Resonance	74

List of Tables (continued ....)

	Page
Table 12: Comparison to Single Particle Estimates in the 1318 Kev Resonance	77
Table 13: Identification of the Peaks in the Ge(Li) Spectrum for the 1416 Kev Resonance	79
Table 14: Comparison to Single Particle Estimates in the 1416 Kev Resonance	83

## CHAPTER 1

### INTRODUCTION

#### 1.1 General

There is a region in the centre of the s-d shell ( $A = 16$  to  $40$ ) around  $A = 19$  to  $31$ , in which the energy levels of most nuclei show definite collective properties. It has been shown (Ollerhead, 1968) that  ${}_{12}\text{Mg}^{24}$  is one of these nuclei and possesses definite rotational and vibrational collective effects in its energy levels.

Due to the fact that  ${}_{12}\text{Mg}^{24}$  is well clear of any shell closures, it might be expected that its properties will not be explained by simple shell model theory. In particular, the reduced gamma radiation widths of its levels are expected to be well below single particle estimates except, possibly, in the case of an electric quadrupole transition in a rotational band where considerable enhancement may occur.

Much work has been done in studying the properties of  ${}_{12}\text{Mg}^{24}$ , a summary of which can be found in Endt and Van der Leun, 1967. A large amount of this work has been carried out using the proton capture reaction on  ${}_{11}\text{Na}^{23}$ , and the main contributors to this work, as far as energies, branching ratios and transition widths of  ${}_{12}\text{Mg}^{24}$  are concerned are

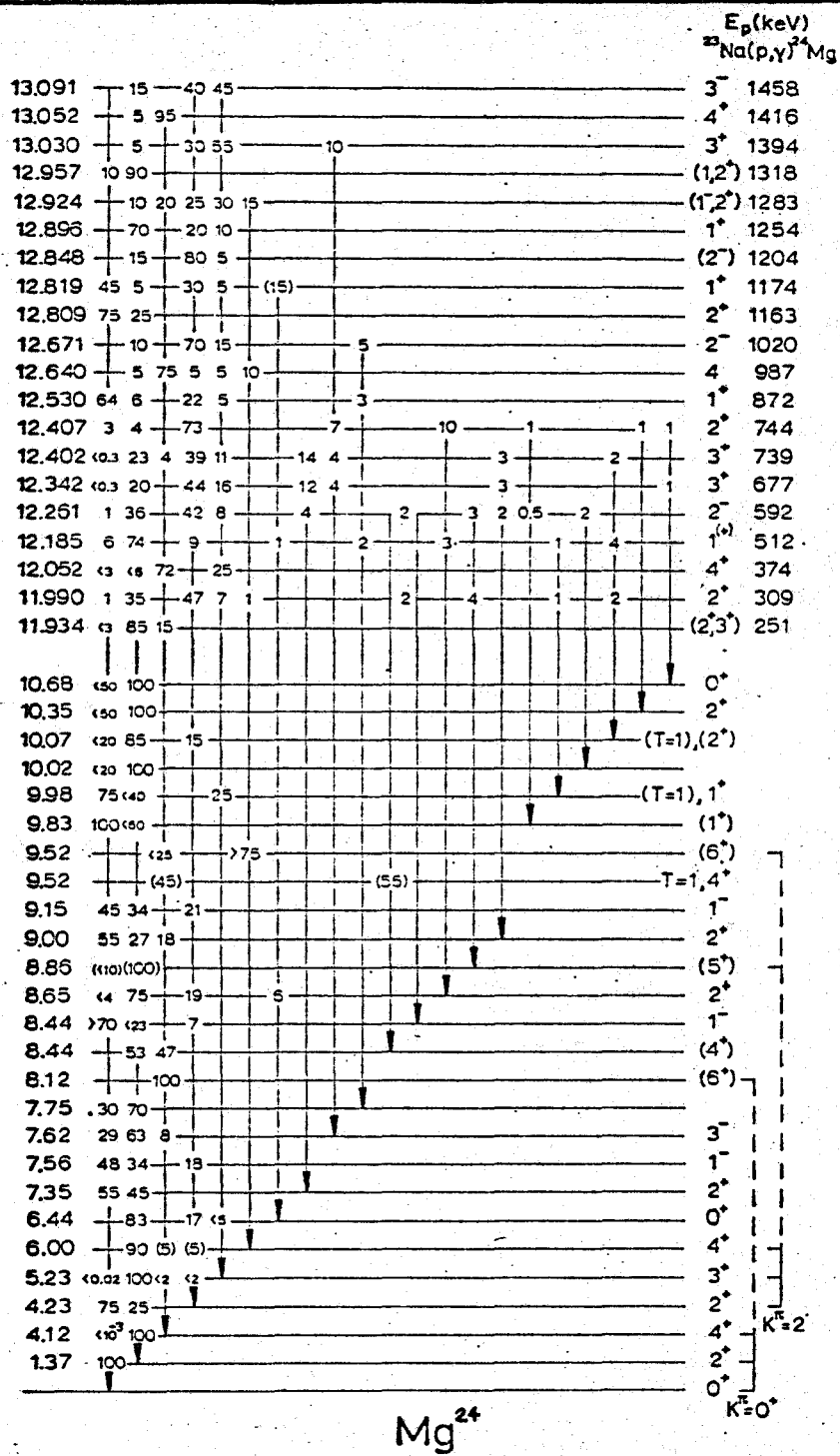


FIG. I. DECAY SCHEME FOR  $Mg^{24}$ .

$E_p$ (Kev)	$E_x$ (Mev)	$\Gamma$ (Kev)	$(2J+1)\Gamma_p \Gamma_x / \Gamma$ (in ev)				$\Gamma_p / \Gamma$
			$\gamma$	$p_1$	$\alpha_0$	$\alpha_1$	
250.9	11.934	<0.02	0.005		<0.01		
308.9	11.990	<0.02	2.2		<0.01	0.3	
374.3	12.052	<0.02	0.05		0.03		
512.1	12.185	<0.05	1.8		<0.2	<0.02	
591.6	12.261	0.64			330	0.8	0.9
592.0	12.261	<0.06	1.7				
676.7	12.342	<0.07	5.6		<0.4	<0.06	
738.9	12.402	<0.09	1.3	0.3	<1.1	1.6	
743.8	12.407	<0.1	1.6	0.3	70	0.35	
872.4	12.530	7.5	9.6	0.2		<1.6	$\geq 0.9$
987.0	12.640	<0.4	4.5	0.2		<1.6	
1010.0	12.662	0.4	<0.9	10	+	110	
1020.4	12.671	5.0	14	130		31	0.9
1163.3	12.809	1.2	2.9	26	+	370	
1173.8	12.819	3.4	13	18		22	0.7
1204.1	12.848	0.3	1.0	5.4		3.5	
1210.0	12.854	0.4	<0.8	19		190	0.7
1254.0	12.896	0.4	1.2	14		310	0.5
1283.6	12.924	5.2	7.2	2200	+	31	>0.9
1318.3	12.957	1.4	53	36		61	
1327.5	12.966	2.7	<0.2	1200		690	
1394.4	13.030	0.7	24	230		27	0.7
1416.8	13.052	<0.2	42	100	+	68	
1458.0	13.091	7.5	12	3750	+	340	0.9

TABLE I: Transition Widths for  ${}_{11}\text{Na}^{23} + p$  Resonances

Anderson (1961), Glaudemans and Endt (1962), Prosser (1962), Nordhagen (1964), and Mourad (1967).

Excluding the work contained in this thesis, an energy level scheme of the work completed at present on  ${}_{11}\text{Na}^{23}(p,\gamma){}_{12}\text{Mg}^{24}$ , together with branching ratios, is shown in Fig. 1, and a table of the known transition widths of these levels is shown in Table 1.

It should be pointed out that until now all  ${}_{11}\text{Na}^{23}(p,\gamma){}_{12}\text{Mg}^{24}$  work has been carried out with NaI(Tl) detectors. It was, therefore, proposed that a study of some of the resonances in  ${}_{11}\text{Na}^{23}(p,\gamma){}_{12}\text{Mg}^{24}$  reaction be made with available semiconductor, Ge(Li), counters, with the object of checking existing data on decay schemes, branching ratios and gamma transition widths, with the much increased resolution possible with these detectors.

This study was made between incident proton energies,  $E_p$ , of 0.5 Mev and 1.8 Mev on the KN Van de Graaff accelerator of the Ontario Cancer Institute in Toronto. The Q-value of the reaction being 11.69 Mev, this range of proton energies excites energy levels in  ${}_{12}\text{Mg}^{24}$  from  $E_x = 12.17$  Mev to 13.42 Mev.

CHAPTER 2  
EXPERIMENTAL METHODS

2.1 Experimental considerations

(i) Introduction

The proton capture experiments discussed in this thesis were carried out using a High-Voltage Engineering Corporation, Model KN, Van de Graaff, capable of giving a beam of protons up to energies around 3 Mev. Energy stabilization of the ion beam was accomplished by utilizing a 25° deflecting magnet and slit system. A nuclear magnetic resonance system was used to measure the magnetic field.

The energy spread of the proton beam, at the target, under normal operating conditions of  $E_p$  approximately equal to 1 Mev was shown by Charlesworth (1967) to be  $\leq 1$  Kev.

Since the accelerator and detector area were in a single room, the target chamber and detector system were located in a concrete blockhouse to reduce the amount of radiation coming from sources other than the immediate target area. This procedure, of course, increases the "signal to noise ratio", leading to the detection of lower intensity radiation than would have been possible without this shielding.

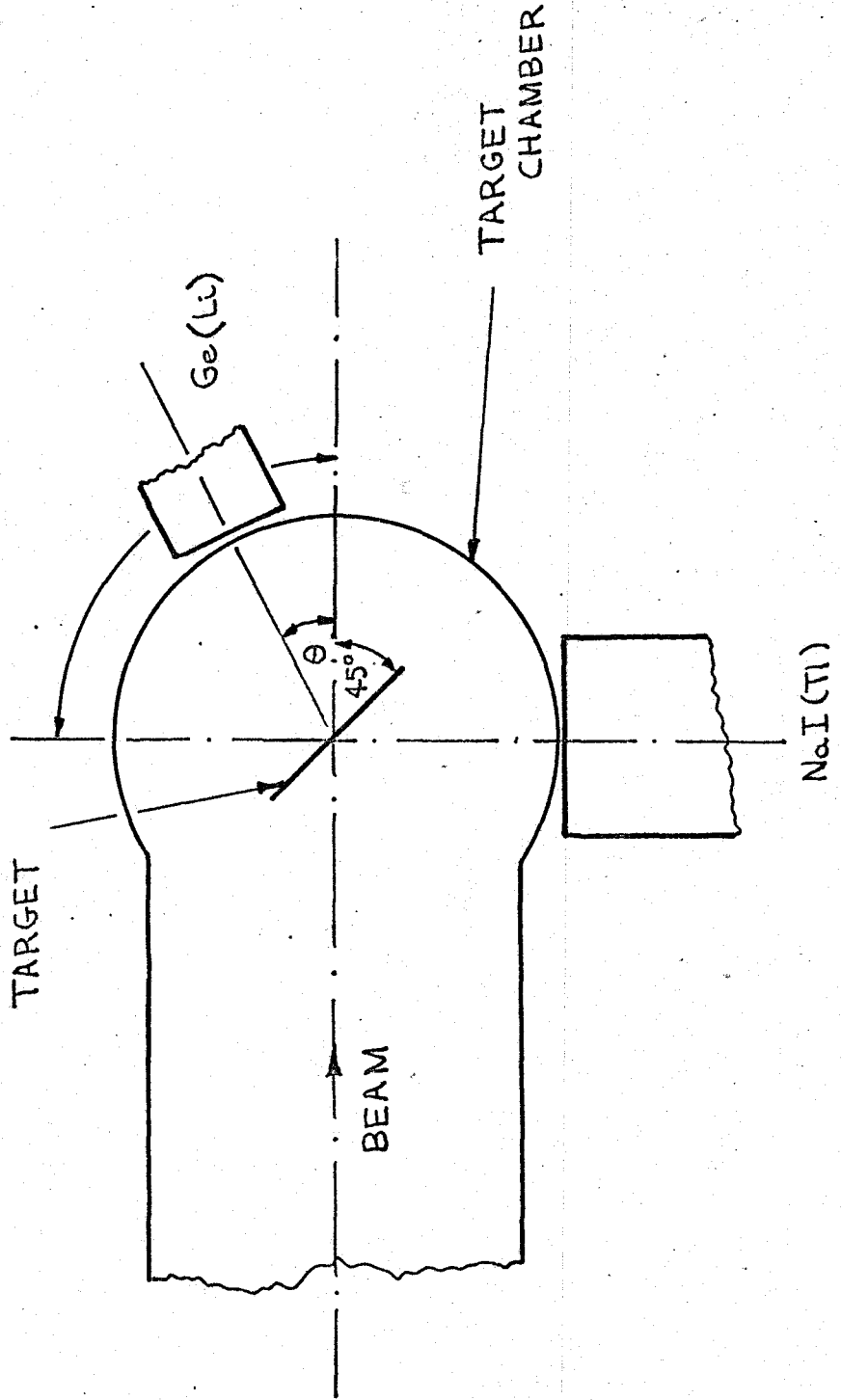


FIG.2. EXPERIMENTAL GEOMETRY.

The Ge(Li) detector used had an effective volume of 40 cu. cm. and was made by the RCA Corporation.

The NaI(Tl) detector used was a 5" by 4" crystal.

(ii) Geometry considerations.

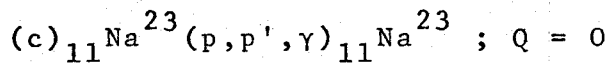
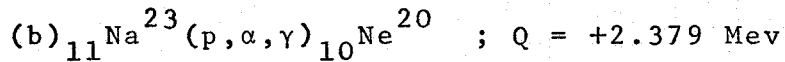
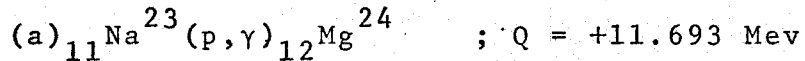
The geometrical layout of the experiment is shown in Fig. 2. The Ge(Li) counter was allowed to move in the horizontal plane through an angle,  $\theta$ , from  $0^\circ$  to  $90^\circ$ , with respect to the beam axis, while the NaI(Tl) counter remained at a fixed angle at all times. The target was placed at  $45^\circ$  to the beam so that gamma-rays from the reaction would pass through a minimum of target backing before reaching the Ge(Li) and NaI counters. The target chamber was so constructed that water cooling could be applied directly to the base of the target. In this experiment targets were used that evaporated at fairly low temperatures, e.g. around  $700^\circ\text{C}$  at atmospheric pressure, and this necessitated the use of water cooling in order to be able to use useful beam currents, e.g. a few microamps, without the targets becoming excessively hot.

In the setting up of the experiment great care was taken to ensure that the proton beam passed through the vertical axis of the target chamber, and that the detectors were at the same horizontal level as the beam at all times. Further, it was ensured that the Ge(Li) counter remained the same distance from the target chamber wall at all angles of  $\theta$ .

Therefore, provided that the beam spot diameter was kept small compared to the detector size, e.g. about 1/8 inch to 1/4 inch in this case was satisfactory, then the geometrical errors in carrying out angular distribution experiments could be kept to a negligible level.

(iii) Electronics considerations.

It must be pointed out that the action of protons on  ${}_{11}\text{Na}^{23}$  can result in three reactions:-



The  ${}_{11}\text{Na}^{23}(p,\alpha,\gamma){}_{10}\text{Ne}^{20}$  reaction is characterised by a strong 1.63 Mev gamma ray from the first excited state of  ${}_{10}\text{Ne}^{20}$ , and the  ${}_{11}\text{Na}^{23}(p,p',\gamma){}_{11}\text{Na}^{23}$  reaction is characterised by a strong 0.44 Mev gamma ray from the first excited state of  ${}_{11}\text{Na}^{23}$ . As will be seen later we are not interested to any great extent in the  ${}_{11}\text{Na}^{23}(p,p',\gamma){}_{11}\text{Na}^{23}$  reaction, but we are interested to see if the  ${}_{11}\text{Na}^{23}(p,\alpha,\gamma){}_{10}\text{Ne}^{20}$  reaction is a competing process at a  ${}_{11}\text{Na}^{23}(p,\gamma){}_{12}\text{Mg}^{24}$  resonance. Therefore, the gamma ray spectrum from the 5" x 4" NaI(Tl) crystal was fed into two separate, single channel analyzers, the gate of one being set to receive only pulses corresponding to 1.63 Mev gamma rays, and the gate of the other being set

to receive all pulses corresponding to gamma rays of greater than 2 Mev. The "1.63 Mev" gate will obviously enable us to see mainly the  ${}_{11}\text{Na}^{23}(p,\alpha,\gamma){}_{10}\text{Ne}^{20}$  reaction, while the "greater than 2 Mev" gate will enable us to see the gamma rays from any  $(p,\gamma)$  reaction that may be occurring in the target.

The gates of the single channel analyzers were set up using gamma rays of known energy, e.g. the 1.17 Mev and the 1.33 Mev gamma rays from  $\text{Co}^{60}$ . One of the gates was originally set up on one of these gamma rays. A pulse from a pulse generator was then fed into the gate and its pulse height varied until the pulses passed through the set gate. The setting on the pulse generator was then normalized to the energy of whichever gamma ray was being used, without varying the output pulse height. Using the fact that the pulse height from the pulse generator was proportional to its dial setting, the two gates were set up at the energies needed, as stated previously. The output from these two gates were fed into two separate scalars for recording purposes.

The gamma ray spectrum from the Ge(Li) counter was fed via a linear amplifier into 3200 channels of a SKIPP 6400 multichannel analyzer. With the gain of the system set such that the multichannel analyzer would display a spectrum containing all possible gamma ray energies from the

(p, $\gamma$ ) reactions, from approximately 0.5 Mev upwards, the energy calibration of the analyzer was around 4 Kev/channel. This was a convenient calibration as it was found that the resolution of the system as a whole was around 10 to 12 Kev for gamma ray energies from around 0.5 Mev to 14 Mev.

(iv) Target and backing choice.

Initially targets of NaCl were used in the experiment but it was found that there were many competing resonances from  $_{17}\text{Cl}^{37}(\text{p},\gamma)_{18}\text{Ar}^{38}$  and  $_{17}\text{Cl}^{35}(\text{p},\gamma)_{18}\text{Ar}^{36}$  reactions, whose Q-values are 10.243 Mev and 8.506 Mev respectively. NaOH targets were then tried and found to be extremely clean of all reactions except those involving sodium.

As it was impossible at the time to produce self-supporting targets of the above substances, it was necessary to form them on a rigid backing. This backing must be thin to avoid any gamma ray absorption but at the same time must be a good conductor to remove the heat caused by the proton beam.

Originally 0.010 inches thick copper sheet was used for the backing and was found successful up to an energy of around 1 Mev when the background increased sharply due to  $_{29}\text{Cu}^{63}(\text{p},\gamma)_{30}\text{Zn}^{64}$  and  $_{29}\text{Cu}^{65}(\text{p},\gamma)_{30}\text{Zn}^{66}$  reactions. Currents of around 7 microamps could be used on these backings without noticeable target deterioration.

Tantalum backings of the same thickness were then

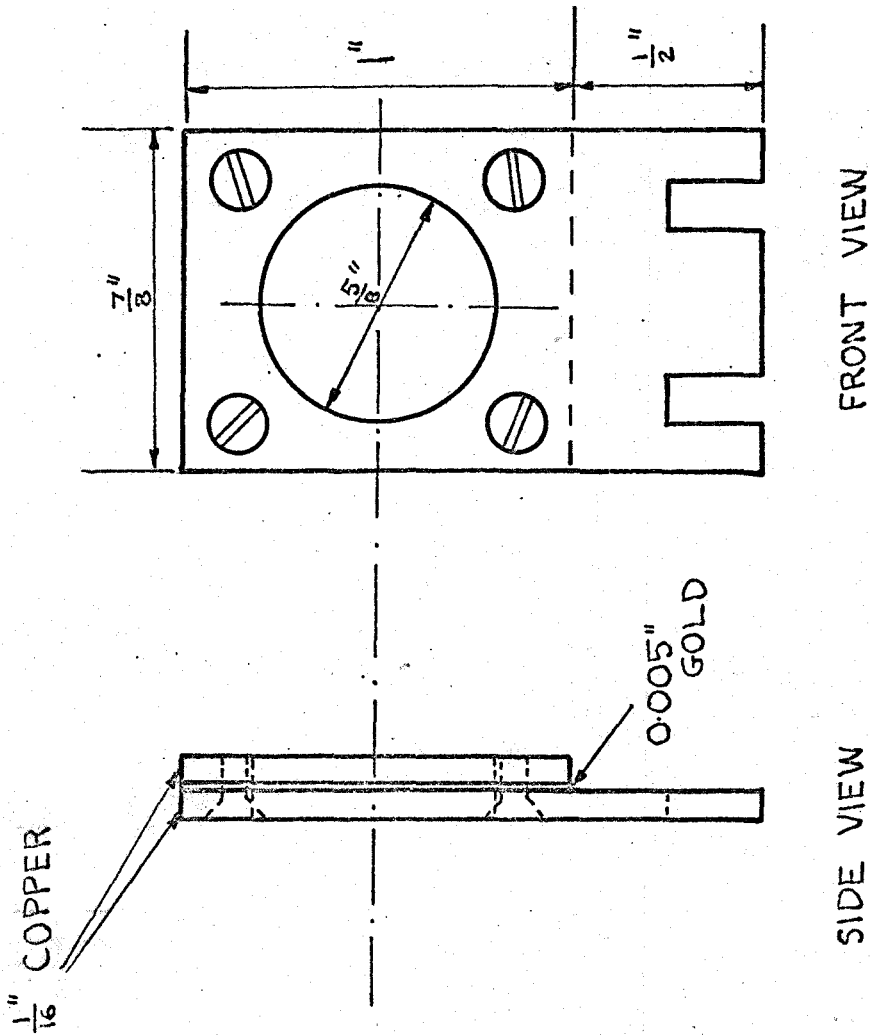


FIG.3. HIGH CURRENT TARGET.

tried and found to be free from excessive background over the whole of the energy range used. However, the current possible was a little less due to the poorer conductivity of tantalum.

In some of the later experiments, it was found that a larger target current would be desirable in order to reduce the amount of running time. For this reason a target backing of 0.005 inches gold was clamped between two pieces of 1/16 inch copper sheet, as shown in Fig. 3. The gold was used because it has the low background property of tantalum with quite a bit better conductivity, together with the fact that it is soft and will make a good thermal contact with the copper supports that are clamping it. The copper supports provide a much more efficient way of conducting heat away from the target than does the usual geometry, hence a much higher current can be used. In this case it was found that currents around 20-25 microamps could be used without excessive damage being done to the target.

However, due to the large amount of copper being exposed to possible stray beam, a tantalum beam stop, with a 3/16 inch hole, was placed a few inches in front of the target. This beam stop was normally grounded to avoid charge build up on it, but, as will be seen later, it could be used for secondary electron suppression by putting about 100 volts, negative with respect to the target on it.

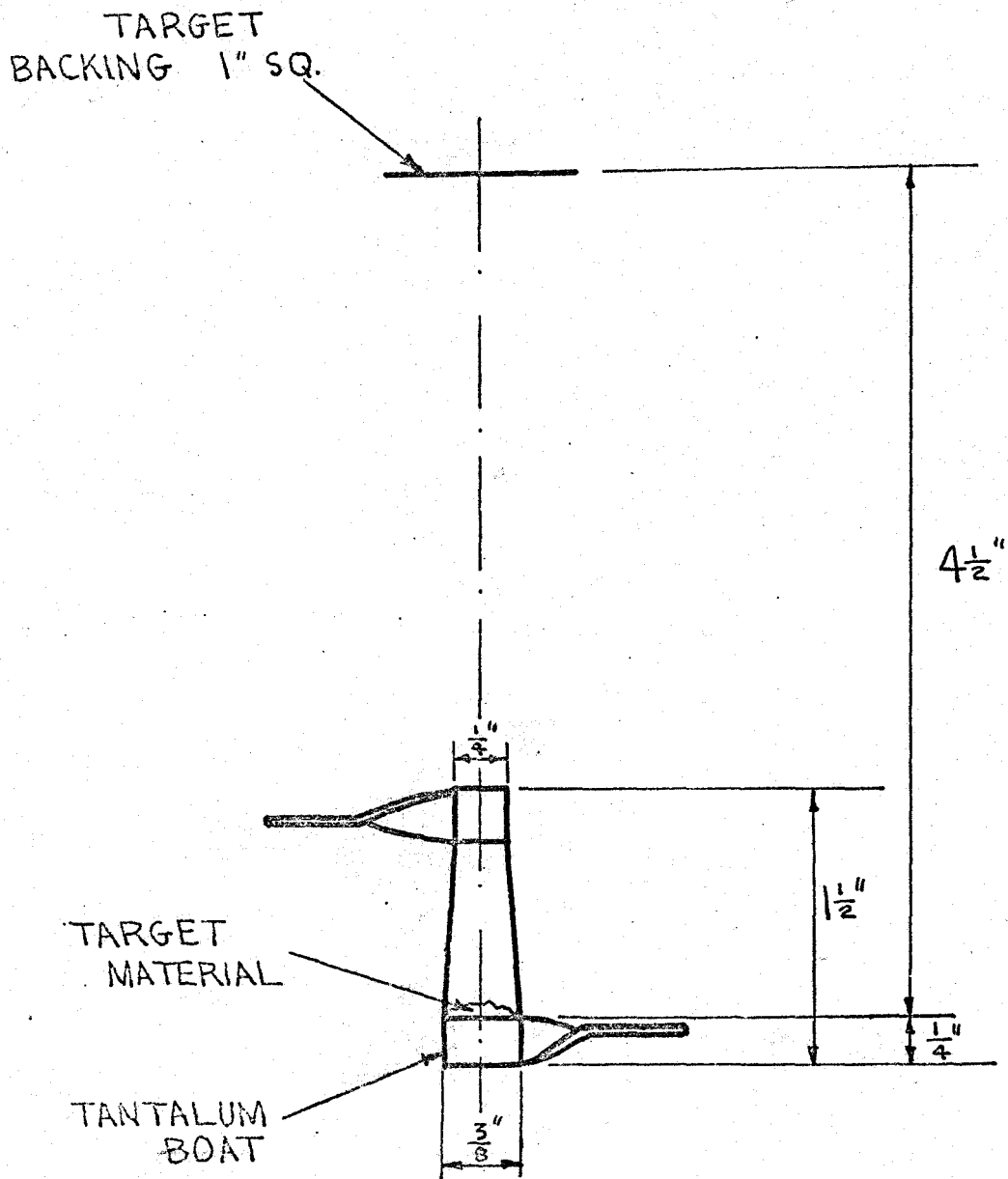


FIG. 4. TARGET EVAPORATION GEOMETRY.

(v) Target and backing preparation.

The copper backings were prepared by first buffing on a workshop buff with fine jewellers polish, and then cleaning in acetone and distilled water.

The tantalum backings were prepared by just washing in acetone and then distilled water.

The gold backings were first cleaned in acetone, then put in an acid bath for several minutes, and, finally, washed in distilled water.

The NaCl and NaOH targets were prepared by evaporation of a certain amount of the substance concerned onto the target backing, in vacuo. The geometry used is shown in Fig. 4. It was found that a target of thickness about 40 micrograms per sq. cm. could be made by evaporating about .5 milligrams of either NaOH or NaCl in the above geometry. This is an energy thickness of around 5 Kev for protons of about 1 Mev.

For high current targets a layer of gold of about one half the thickness of the target was deposited on the top of the target. This was thought to help stop deterioration of the target and indeed seemed to be an improvement on targets without this gold surface.

Both NaCl and NaOH targets were prone to absorbing water if left in the atmosphere for any length of time. The effects on NaCl of water absorption were very little, but the effects on NaOH were quite noticeable, and the latter

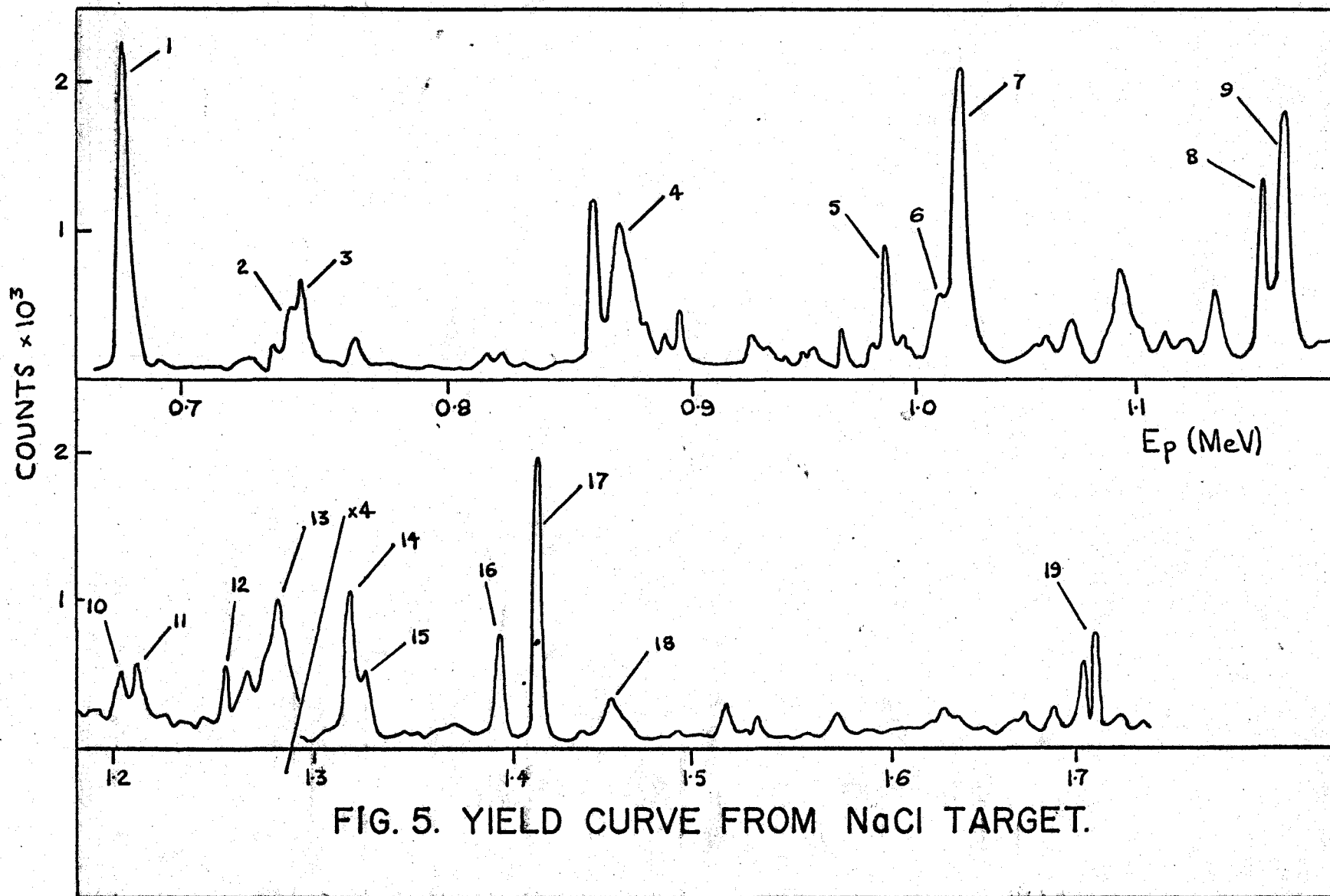


FIG. 5. YIELD CURVE FROM NaCl TARGET.

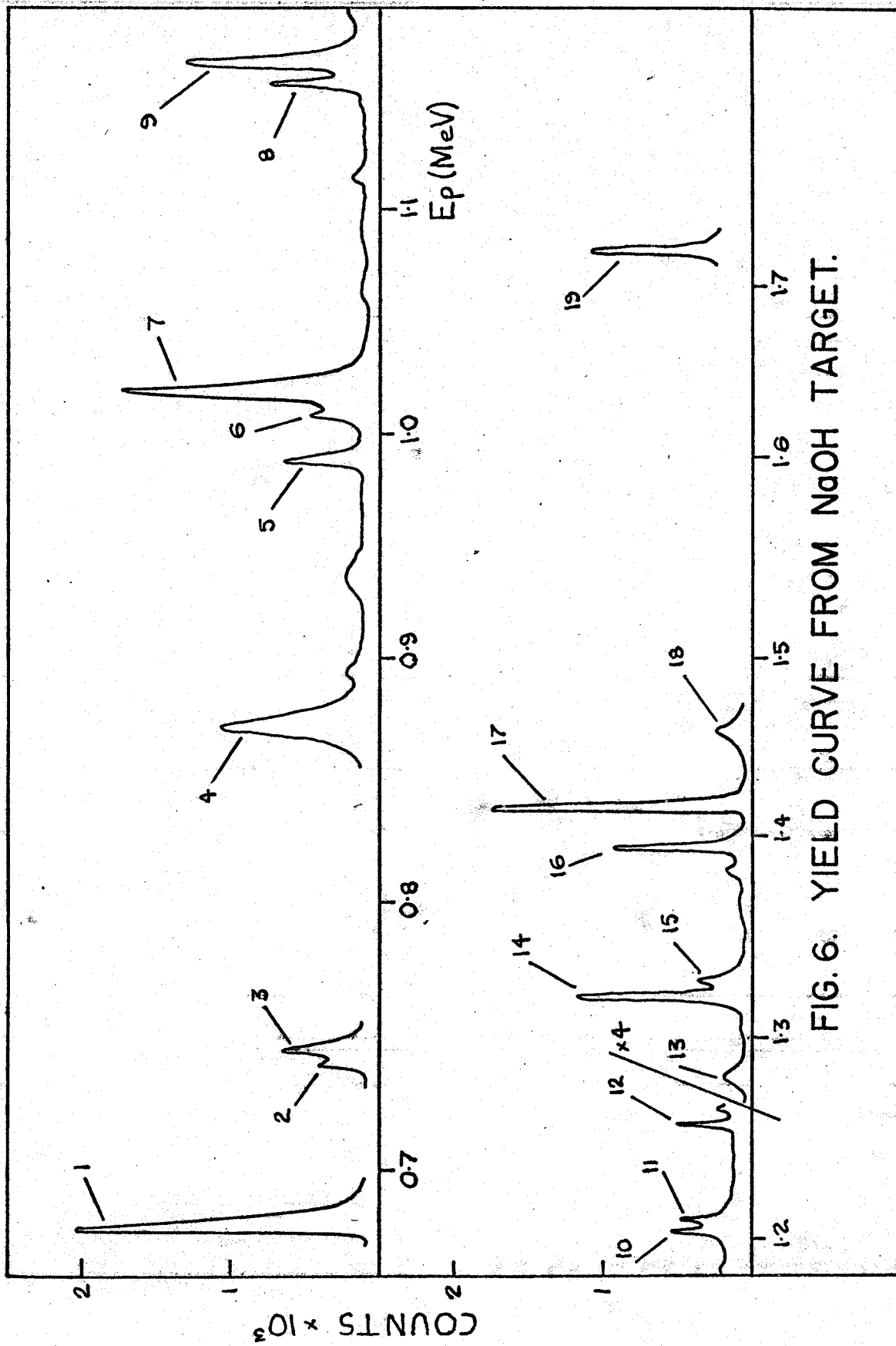


FIG. 6. YIELD CURVE FROM NaOH TARGET.

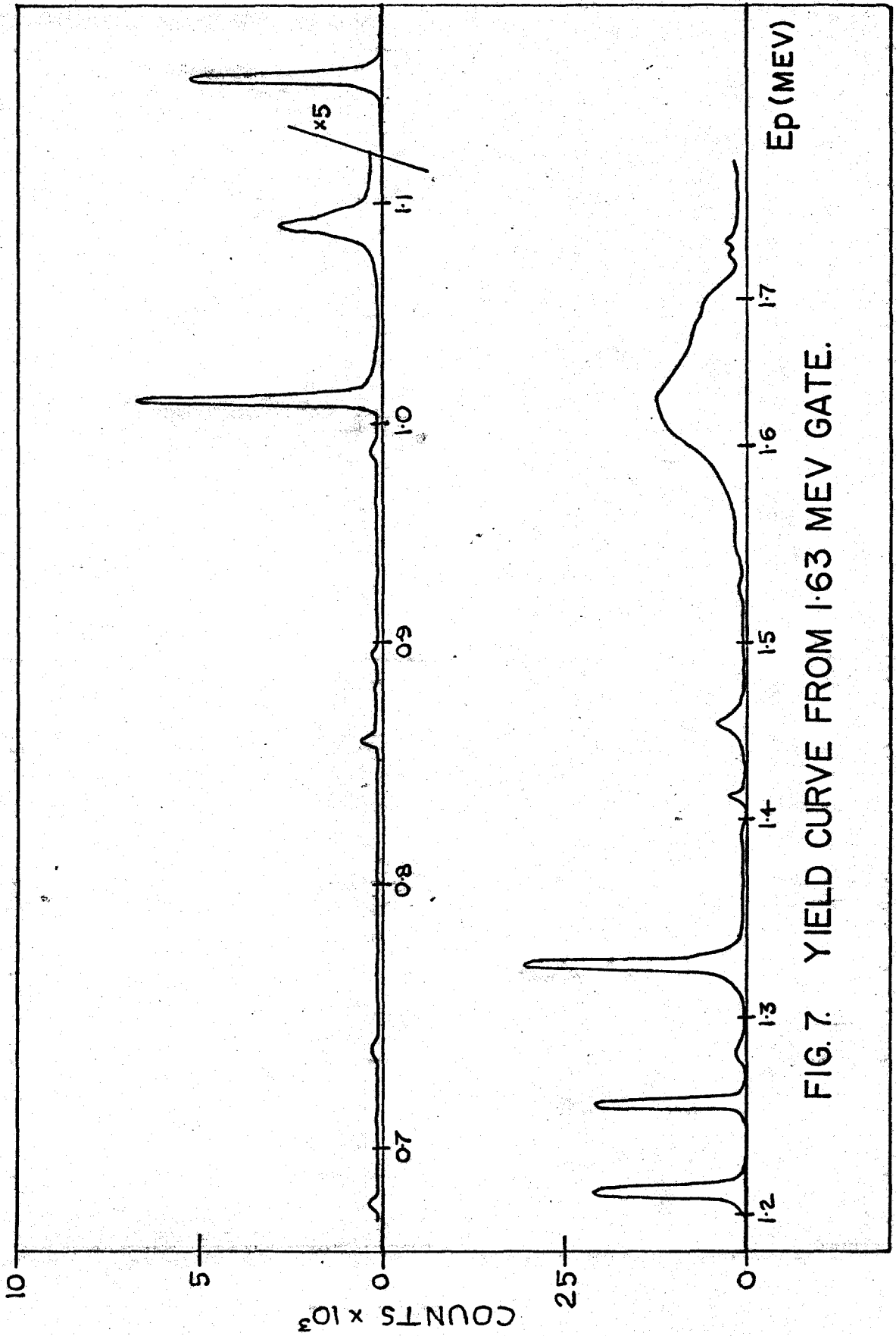


FIG. 7. YIELD CURVE FROM 1.63 MEV GATE.

Resonance Number	Proton Energy (Kev)
1	676
2	739
3	744
4	872
5	987
6	1010
7	1020
8	1163
9	1174
10	1204
11	1210
12	1254
13	1284
14	1318
15	1328
16	1394
17	1417
18	1458
19	1720

TABLE 2: Identification of  $_{11}\text{Na}^{23}(p,\gamma)_{12}\text{Mg}^{24}$  Resonances

targets had to be handled with extreme care so as not to expose them to the atmosphere for too long. This handling involved letting the vacuum evaporating system up to atmosphere with dry nitrogen, and, also, putting the target into the target chamber in an atmosphere of dry nitrogen. At all other times the target was in an evacuated desiccator.

## 2.2 Yield curve considerations

In the initial work measurements of the gamma ray yield corresponding to the "1.63 Mev" and "greater than 2 Mev" gates were made for the proton energy range from  $E_p = 0.5$  Mev to  $E_p = 1.8$  Mev. This was in order to find the  ${}_{11}\text{Na}^{23}(p,\gamma){}_{12}\text{Mg}^{24}$  resonances and the contribution to these resonances from the  ${}_{11}\text{Na}^{23}(p,\alpha,\gamma){}_{10}\text{Ne}^{20}$  reaction.

Yield curves were obtained for both NaCl and NaOH targets. The yield curves from the "greater than 2 Mev" gate for NaCl and NaOH are shown in Fig. 5 and Fig. 6 respectively. A yield curve from the "1.63 Mev" gate, when a NaOH target was used, is shown in Fig. 7.

All the resonances that had been seen in previous work in this energy range were seen, and a new resonance that had not been seen previously was found at around 1.72 Mev.

The resonances shown in the above curves are numbered and the numbers are explained in Table 2. The energy thickness of the targets used for these yield curves was around

5 Kev at  $E_p \sim 1$  Mev.

### 2.3 Procedure for finding decay schemes

For finding the decay scheme of a particular resonance, gamma ray spectra from the Ge(Li) counter were obtained at  $0^\circ$  and  $90^\circ$ . It should be pointed out that if the lifetime of a resonance level is much smaller than the time the recoil nucleus takes to slow down, then the energies of the gamma rays observed at  $0^\circ$  to the beam direction will show a significant increase in energy over the true gamma ray energy. This is due to the Doppler shift effect of a gamma ray being emitted from a moving nucleus. Of course, no Doppler shift will be seen at  $90^\circ$  to the beam direction.

It should be pointed out that with the high excitation energies achieved in this reaction, it is reasonable to expect, in the proton energy range studied, to find some resonances with lifetimes much shorter than the recoil time of the nucleus concerned. As will be seen from a subsequent section on measurements of gamma radiation widths, the resonances with the largest gamma ray yields will have the largest resonance strengths,  $\omega\gamma$ . This, in turn, means that these resonances will have the largest total widths and the shortest lifetimes. Therefore, by choosing to study only the resonances with the largest gamma ray yields, it is most probable that the energies of the primary gamma rays from the resonances will exhibit the full Doppler shift.

Subsequent decays in the cascades from these resonances may or may not exhibit Doppler shift effects. The magnitude of the Doppler shift effect seen in these subsequent decays will, of course, depend on the lifetimes of the intermediate states.

In the resonances studied in this thesis, typical Doppler shifts on the primary gamma rays were around 15 to 20 Kev for a 12 Mev gamma ray. For this reason the true energies of the gamma rays were found from the  $90^\circ$  run while the  $0^\circ$  run served to detect the primary gamma rays in some cases. The energies of the peaks in the  $90^\circ$  spectrum will be given by  $E_\gamma = A(x + B)$ , where  $E_\gamma$  is the energy deposited in the detector,  $A$  is the dispersion of the analyzer, i.e. Kev/ch.,  $A \cdot B$  is the energy corresponding to channel zero, and  $x$  represents the analyzer channel number.  $A$  and  $B$  are constants in this equation.

Values of  $A$  were found at many points in the spectrum from the fact that the 2nd escape and 1st escape, and 1st escape and full energy peaks, of any particular incident gamma ray, are separated by exactly 511 Kev. By knowing the number of channels separating these peaks,  $A$  can be found. From these values of  $A$  an average value of  $A$  was estimated so as to cover the whole of the spectrum. Knowing  $A$  and using the accurately known full energy peak of the 1.369 Mev gamma ray in the spectra as a standard, the energies of all the other

peaks in the spectrum were found by using the formula mentioned earlier in this section.

In cases where a definite non-linearity was present in A over the spectrum, the energies of the peaks were found by using the values of A appropriate to the various sections of the spectrum.

Obviously in order to get accurate values of A, the channel numbers of the peaks concerned must be known accurately. For this reason the centroid of each peak was found using the formula:-

$$\text{Centroid} = \frac{\sum \text{ch. nos.} \times \text{counts}}{\sum \text{counts}}$$

This technique allowed the finding of the channel number of a peak, in a typical case, to about 1/10th of a channel.

In order to facilitate calculations and not to have to work out the energy of every single peak in the spectrum, the full energy, 1st escape and 2nd escape peaks for each particular gamma ray were identified and the energy of the largest of these three peaks was found. The necessary correction was then made in order to give the full energy of the gamma ray concerned.

Once the full energy values for all the gamma rays were known, these were fitted to a decay scheme by requiring that the sum of the gamma ray energies in a particular

cascade be equal to the resonance energy. After a plausible decay scheme had been found the dispersion,  $A$ , was altered slightly, if necessary, to give the maximum self-consistency between the energies of all the gamma rays, so that the most accurate decay scheme was found.

As an added check on the decay scheme found by the above technique, the intensities of the gamma rays in each proposed cascade were found, using the technique described in the next section, and checked for consistency.

#### 2.4 Procedure for finding branching ratios

In the geometry used in this experiment the intensity of a gamma ray in a certain transition, recorded in the Ge(Li) counter, at a certain angle  $\theta$ , with respect to the beam axis, is given by the expression:-

$$W(\theta) = \sum_n A_n P_n (\cos \theta)$$

where the summation is only over even values of  $n$ .

Now if this expression is integrated over  $4\pi$  solid angle, we obtain:-

$$\int_{4\pi} W(\theta) = \text{constant} \times A_0$$

It can be seen, therefore, that  $A_0$  will be proportional to the total number of gamma rays occurring in that transition, during the time taken to run the experiment.

There is, however, a correction in the above equation

due to the finite solid angle that the detector makes with the beam spot. This property tends to 'smear out' angular distribution effects. It is more strictly true to write:-

$$W(\theta) = \sum_n Q_n A_n P_n (\cos \theta)$$

where  $Q_n$  is an attenuation coefficient that depends only on the solid angle that the detector makes with the beam spot, and is a constant for any particular gamma ray energy. In the case of  $A_0$ , however,  $Q_0$  can be set to unity as  $A_0$  does not depend on any angular effects.

If, therefore, the  $A_0$  coefficients could be found for all the observed transitions from a particular energy level, then, by a relative comparison of these values, the branching ratios of the gamma rays from that particular level could be found.

Of course, there would have to be a correction made to each  $A_0$  value for the efficiency of that particular energy gamma ray in the detector used. For this reason some time was spent on producing a relative efficiency curve for the 40 cu. cm. Ge(Li) counter used in these experiments. Details of the production of this relative efficiency curve will be given in a later section.

In order to find the  $A_0$  value for any particular gamma ray transition, it was decided to record Ge(Li) spectra, from the resonance concerned, at several different angles of

$\theta$ , and then least squares fit the intensity of the particular gamma ray at each angle to the Legendre Polynomial expansion mentioned at the beginning of this section. It was assumed that no higher multipole radiation than quadrupole would be present in any gamma ray transition and, therefore, the fit only included terms up to  $n = 4$  in the expansion.

Before the spectra, obtained at the various angles of  $\theta$ , for the resonance concerned, can be used in a relative calculation there is a question of normalizing each run to a common incident proton number. This normalization was initially performed by using the total counts appearing on the scalar registering the pulses from the NaI(Tl) crystal passing through the "greater than 2 Mev" gate during the time of the particular run. It was assumed that the number of incident protons would be directly proportional to this scalar count. This assumes that the height of the yield curve over the resonance in question and the background contribution to this yield curve remains constant over the time taken to perform the series of runs at all angles. This was checked by plotting yield curves over the particular resonance at regular intervals during the runs. However, inaccuracies could arise in this method of normalization if the gain of the NaI(Tl) system fluctuated during runs. This effect was thought to be small.

In later experiments with high proton currents, some changes in yield curve shape was noticeable over the length of a run. In this case the above type of normalization becomes quite inaccurate. To ensure an accurate normalization for these experiments it was decided to record a gamma ray spectrum from the fixed angle NaI(Tl) crystal during each run on the Ge(Li) counter. The normalization was then achieved by normalizing the areas under a particular peak on the NaI(Tl) spectrum. Due to the poor resolution of NaI(Tl), the area under each peak concerned was found by calculating the centroid of the peak, as explained previously, and then summing the counts in a fixed number of channels either side of the centroid. It was necessary to correct this number of channels from spectrum to spectrum if the gain of the system changed appreciably between runs. Subtraction of background proved unnecessary as the normalization coefficients changed by less than 1/2% when this was done.

Now, after normalization, the relative intensities of the particular gamma ray under study in the Ge(Li) spectrum at each angle used, will be equal to the relative areas under the 2nd escape, 1st escape, or full energy peak of that particular gamma ray. Obviously for the best statistics, the largest of these three peaks was used to find the angular distribution of the gamma ray concerned.

The areas under these peaks were found by summing the

counts in all channels contained in the peak and then subtracting from this total the background contribution to the peak. Generally, the level of the background under the peak could be assessed by observing the level of the background for twenty to thirty channels above and below the peak, and assuming that no drastic background change occurs directly under the peak. In this case the errors on these areas are given by the statistical factor, (Feynman, 1963),

$$\begin{aligned}
 \Delta Y &= [\text{Variance (YIELD)}]^{1/2} \\
 &= [\text{Variance (TOTAL COUNTS - BACKGROUND COUNTS)}]^{1/2} \\
 &= [\text{Variance (TOTAL COUNTS)} + \text{Variance (BACKGROUND)}]^{1/2} \\
 &= [\text{Variance (YIELD)} + 2 \times \text{Variance (BACKGROUND)}]^{1/2} \\
 &= [\text{YIELD} + 2 \text{ BACKGROUND}]^{1/2}
 \end{aligned}$$

In some cases, however, it was quite difficult to assess the level of the background. In these cases an intelligent guess was applied and a corresponding possible error on this guess was included into the final calculation.

The  $A_0$  values found from the above calculations are just those of the 2nd escape, 1st escape or full energy peaks, whichever was used to find the angular distributions of the incident gamma ray concerned. Therefore, the correction for the efficiency of the Ge(Li) counter must be obtained from the appropriate relative efficiency curve, e.g. the 2nd escape, 1st escape, or full energy curve, as shown

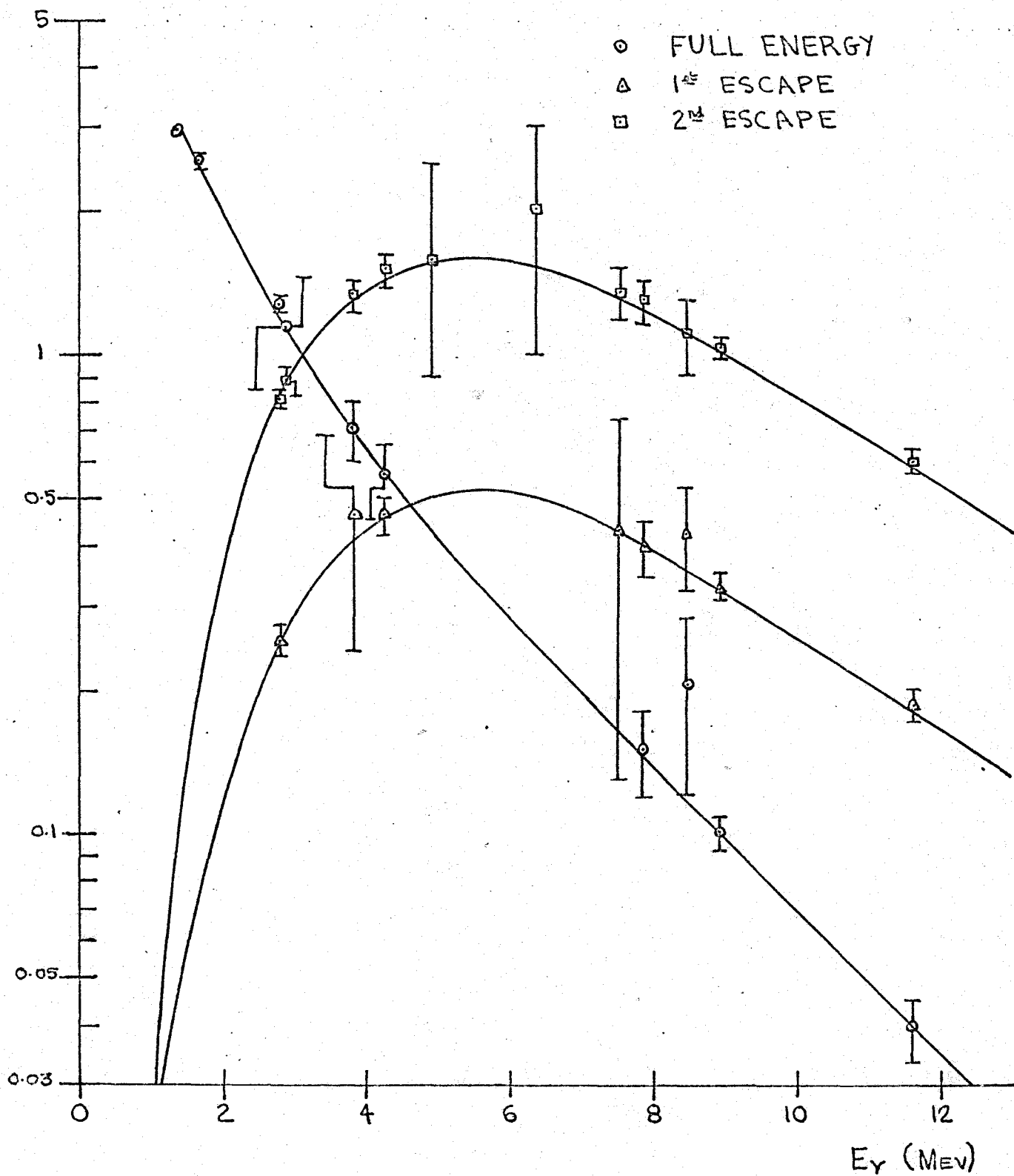


FIG.8. RELATIVE EFFICIENCY CURVE FOR Ge(Li)

in Fig. 8.

In cases of weak transitions where statistical errors are quite large, the  $A_0$  values for a particular transition may be found from the areas under the peaks in the  $55^\circ$  spectrum only. This is because  $P_2(\cos 55^\circ) = 0$  and it is reasonable to assume that the  $A_4$  coefficient will be small compared to the  $A_0$  coefficient.

### 2.5 The Ge(Li) detector relative efficiency curve

As has been previously mentioned, there is a necessity to know the relative efficiency curve of the Ge(Li) detector used in these experiments. The relative efficiency curve can be found by three main methods:

- (a) By using known radioactive sources of known strengths.
- (b) By a relative calibration from a known efficiency curve of another detector.
- (c) By using a 100% or near 100% gamma ray cascade from a known nucleus.

Only the last two methods were employed with the above detector. These two methods are described below:-

(b) In this method the counter with the known efficiency was placed at, say,  $\theta = 90^\circ$  in the same geometry as was used previously. The counter of the unknown efficiency was placed at  $\theta = 0^\circ$ . These two counters then recorded

simultaneously the gamma ray spectrum from a known reaction, in this case the 1020 Kev resonance in the  $\text{Na}^{23}(\text{p}\gamma)\text{Mg}^{24}$  reaction. The counters were then reversed and the same spectrum recorded in a similar fashion. It can be shown that the formula relating the efficiency of these two detectors is:-

$$\epsilon_1 = \sqrt{\frac{N_1(0^\circ)N_1(90^\circ)}{N_2(0^\circ)N_2(90^\circ)}} \epsilon_2$$

where:

$N_1(0^\circ)$  = Nos. of cts. in a certain peak in the spectrum from counter 1 at  $0^\circ$ .

$N_1(90^\circ)$  = Nos. of cts. in the same peak in the spectrum from counter 1 at  $90^\circ$ .

$N_2(0^\circ)$  = Nos. of cts. in the same peak in the spectrum from counter 2 at  $0^\circ$ .

$N_2(90^\circ)$  = Nos. of cts. in the same peak in the spectrum from counter 2 at  $90^\circ$ .

$\epsilon_1$  = efficiency of counter 1 for the peak concerned.

$\epsilon_2$  = efficiency of counter 2 for the peak concerned.

The peak concerned can be a 2nd escape, 1st escape or full energy peak.

This technique, then, nullifies all angular effects of the gamma rays and also the different finite sizes of

the detectors.

The counter of known efficiency was a 23 cc Ge(Li) counter and the points on the efficiency curve found from this method are at gamma ray energies of 1.37 Mev, 1.63 Mev, 2.86 Mev, 3.81 Mev, 4.23 Mev, 4.90 Mev, 6.35 Mev, 7.50 Mev, 7.85 Mev, and 8.44 Mev. The resulting curve was quite good except that the errors on some points were quite large.

(c) In this method, if a cascade is known to be a 100% cascade, then by the angular distribution means explained previously, the  $A_0$  value for each gamma ray in the cascade can be found and compared. Obviously the  $A_0$  values should be equal apart from the efficiency of the detector used in the experiment.

A cascade of this type occurs in the 1318 Kev resonance in the  $\text{Na}^{23}(\text{p}\gamma)\text{Mg}^{24}$  reaction. The cascade is the Res.  $\rightarrow$  1.37  $\rightarrow$  g.s. and this, therefore, will give a relative energy efficiency between the 11.59 Mev and 1.37 Mev gamma rays.

A similar cascade is the 1416 Kev resonance also in  $\text{Na}^{23}(\text{p}\gamma)\text{Mg}^{24}$ . This cascade is the Res.  $\rightarrow$  4.12  $\rightarrow$  1.37  $\rightarrow$  g.s. Now, the Res.  $\rightarrow$  4.12  $\rightarrow$  1.37 cascade is known to be a 100% but the 1.37 Mev level is also fed in small amounts from other levels than the 4.12 Mev. However, this effect can be allowed for as will be shown in the section governing the study of this resonance. This cascade, therefore, yields a

relative efficiency between the 8.93 Mev, 2.75 Mev and 1.37 Mev gamma rays.

The relative efficiencies thus found were normalized to the 1.37 Mev value on the efficiency curve found from the previous technique.

The efficiency curve obtained from the above techniques is shown in Fig. 8 and is fairly accurate except in the region from 4.5 to 7 Mev. However, it was found that very few gamma rays of this energy were seen, and those that were seen were quite weak, and, therefore, accuracy was not so important in these cases.

## 2.6 Procedures for finding gamma transition widths

### $\Gamma_\gamma$

#### (i) Theoretical considerations.

It is well known that the variation of the cross-section of a reaction, over a resonance, is governed by the Breit - Wigner formula, (H.E. Gove, 1959):-

$$\sigma_T(E) = \sigma_R \frac{1/4 \Gamma^2}{(E-E_R)^2 + 1/4 \Gamma^2}$$

$$\text{where } \sigma_R = \frac{4\pi \lambda^2 \omega_\gamma}{\Gamma}$$

$$\text{where } \omega_\gamma = \frac{(2J_1 + 1)}{(2i_1 + 1)(2I_0 + 1)} \frac{\Gamma_1 \Gamma_2}{\Gamma}$$

The explanation of the terms in the above equation are as follows:-

$E$  = laboratory energy of the input particle

$E_R$  = observed resonance energy

$\Gamma$  = total observed resonance width

= sum of the widths for all the possible decay channels of the resonance

$\Gamma_1$  = the sum of the widths of the observed formation channels of the resonance

$\Gamma_2$  = the sum of the widths of the observed decay channels of the resonance

$J_1$  = spin of the resonance level

$i_1$  = spin of the input particle

$I_0$  = spin of the target nucleus

and  $\lambda = \frac{Ma + M_x}{M_x} \frac{\hbar}{\sqrt{2MaE}}$

where  $Ma$  = mass of incident particle

$M_x$  = mass of target nucleus

In this resonance formula the term of interest is  $\omega_\gamma$ , or the so-called 'resonance strength'. In the case of the  $\text{Na}^{23}(p,\gamma)\text{Mg}^{24}$  reaction, this would be written as:-

$$\omega_\gamma = \frac{(2J_1 + 1)}{(2i_1 + 1)(2I_0 + 1)} \frac{\Gamma_p \Gamma_\gamma}{\Gamma}$$

This 'resonance strength' can be calculated experimentally from the yield curve over the resonance in question.

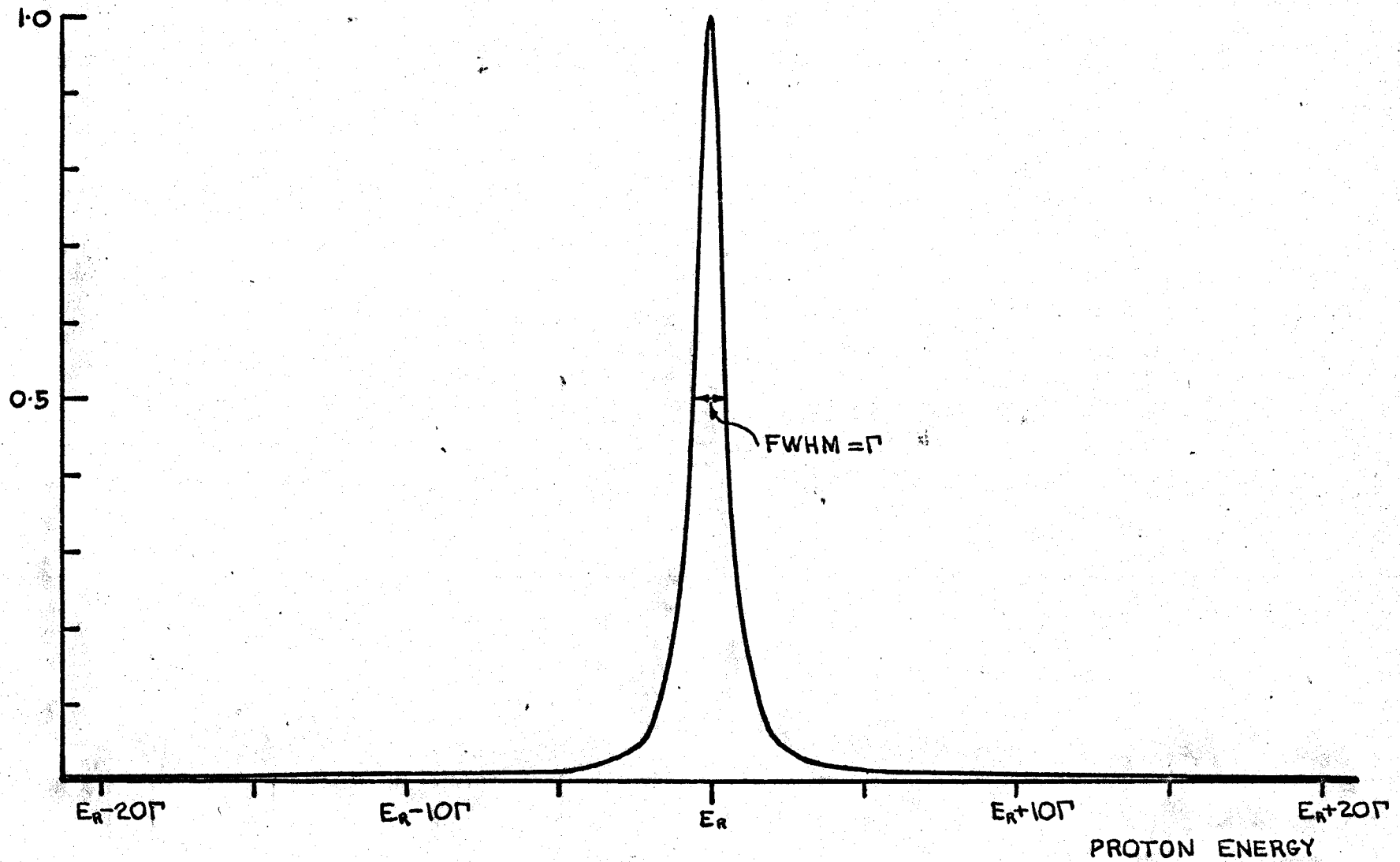


FIG. 9. REACTIONS vs. PROTON ENERGY IN A THICK TARGET.

However, before attempting to derive the formulae relating the yield curve characteristics to the resonance strengths, the reasons for the shape of the yield curve obtained experimentally must first be understood.

In order to explain this more clearly, it is useful to consider the limiting case where a flux of particles of energy  $E \gg E_R$  are incident on a target of energy thickness  $t \gg E$  and  $\gg \Gamma$  for a time  $T$ . By energy thickness it is meant the energy that an incident particle loses in passing through the target.

As the protons, in this case, pass through the target they lose energy by various types of collisions and at some stage their energy will pass into and through the energy range where the probability of a reaction of the type under study will become significant. The probability is obviously governed by the Breit-Wigner cross-section formula for the resonance under study. If, now, a plot were made of the number of reactions of the type under study occurring in time  $T$ , at proton energy  $E$ , vs. the proton energy  $E$ , then the curve would be similar to that shown in Fig. 9. The maximum of the curve shown has been normalized to unity. The curve would have a Breit-Wigner shape with a FWHM equal to the  $\Gamma$  of the resonance under study. This curve will only result if the number of reactions of the type being studied is much less than the incident proton number. This is an

extremely good approximation in the reaction being studied.

By definition,  $\sigma(E)$  is the probability of a reaction, (of the type being studied), per atom (in which the reaction is occurring), per  $\text{cm}^2$  per incident proton of energy  $E$ . Consider now a thin element, width  $dE$ , in the above curve. The number of atoms per  $\text{cm}^2$  that the proton 'sees' when it passes through this energy range will be:-

$$= \frac{dE}{k(E)} \text{ atoms/cm}^2$$

where  $k(E)$  is the energy lost by the proton per atom (in which the reaction is occurring) per  $\text{cm}^2$ . This is usually referred to as the atomic stopping cross-section of the element concerned.

It can now be seen that the number of reactions, of the type under study, occurring in the energy range  $dE$ , at proton energy  $E$ , will be:-

$$= \sigma(E) \frac{dE}{k(E)} N$$

where  $N$  = total number of protons incident on the target in the time  $T$ .

Therefore, the total number of reactions of the type under study, occurring in the whole of the target will be:-

$$Y(\infty) = N \int_0^{\infty} \sigma(E) \frac{d(E)}{k(E)}$$

The justification in integrating from 0 to  $\infty$  arises from the fact that the Breit - Wigner curve is a rapidly decreasing function on either side of its maximum. To illustrate this fact consider the following figures for various target thicknesses and incident proton energies:-

<u>Target thickness</u> (t)	<u>Incident</u> <u>proton energy</u> (E <sub>b</sub> )	<u>Y(t)</u> <u>Y(∞) × 100%</u>
40Γ	E <sub>R</sub> + 20Γ	98.4%
20Γ	E <sub>R</sub> + 10Γ	96.8%
10Γ	E <sub>R</sub> + 5Γ	93.6%
5Γ	E <sub>R</sub> + 2.5Γ	87.5%

It should be noted that the figures are given for incident proton energies that give the proton energy,  $E = E_R$ , at an energy depth of  $t/2$  into the target. This is, of course, the incident proton energy that will give the maximum number of reactions possible in a target of thickness  $t$ .

It should also be pointed out that in the above calculations  $k(E)$  has been assumed to remain constant with energy. This is a good approximation as the values of  $\Gamma$  are typically the order of a few Kev at most, and the  $k(E)$  value in the targets used vary by about 1% in 20 Kev at proton energies around 1 Mev.

Consider now a target of energy thickness  $40\Gamma$  for example. If the incident proton energy is varied such that it

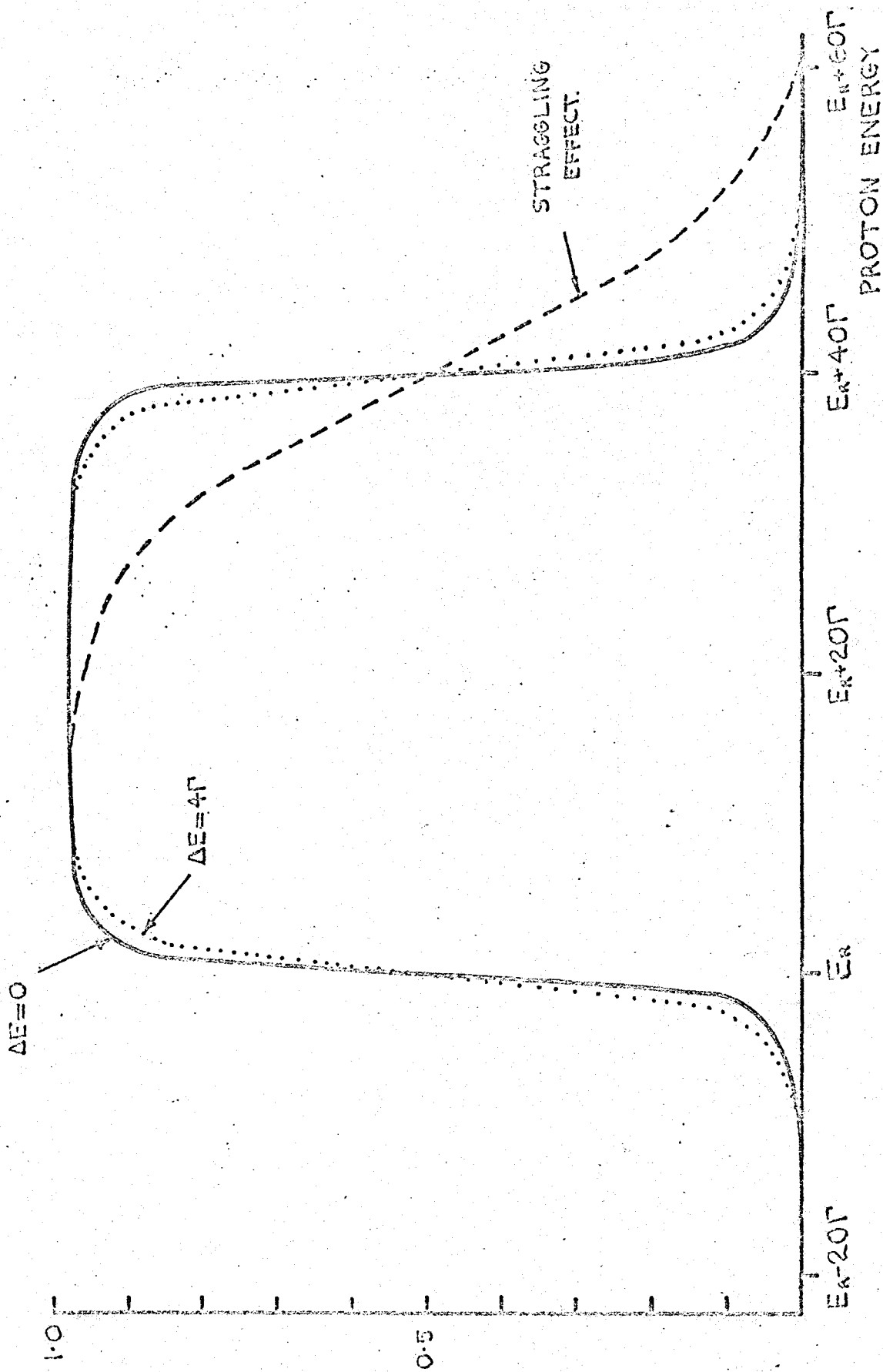


FIG.10. THEORETICAL YIELD CURVES.

covers a range of energies from well below the resonance energy to well above it, and a plot made of the total number of interactions occurring at each incident energy vs. incident energy, then the curve shown in Fig. 10 will result. Obviously, the number of reactions occurring at each incident energy will be proportional to the area under that part of the curve shown in Fig. 9 that the energy of the incident proton covers on slowing down in the target. The curve shown in Fig. 10 is what is termed the yield curve over the resonance in question. The points on the curve shown are normalized to the  $Y(\infty)$  value for the  $\Gamma$  concerned. It can be seen from this curve that the energy of the resonance occurs halfway up the lower energy edge of the curve. It can also be seen that the height of the step in this curve is, to a good approximation, equal to  $Y(\infty)$ . Therefore, knowing the height of this step, then the resonance strength,  $\omega\gamma$ , can be found.

The fact that the yield curve shown in Fig. 10 does not look exactly like yield curves found by experiment is due to two main reasons. One reason is that in all the preceding arguments a mono-energetic beam of protons has been used, whereas experimentally there is always a finite energy spread in a beam of particles from a Van de Graaff accelerator. The energy distribution in the beam is such that it can be assumed Gaussian, and, therefore, a rapidly varying function on either side of its maximum. This incident beam

energy spread will alter the shape of the high and low energy edges of the yield curve. However, unless the beam energy spread together with  $\Gamma$  is appreciable compared to the target thickness, very little decrease in the height of the yield curve will result. The dotted line in Fig. 10 shows the effects on that particular yield curve of an incident beam energy spread,  $\Delta E$  (FWHM) =  $4\Gamma$ . Even if  $\Delta E = 10\Gamma$ , the height of this yield curve would decrease by less than 1%.

The second contribution to the difference between the theoretical and experimental yield curves is caused by the energy straggling of the protons as they pass through the target. This effect is obviously going to make the slope of the high energy edge of the yield curve much less than that of the low energy edge. As a typical example, if  $\Gamma$  in the yield curve shown = 0.5 Kev, i.e.  $\Delta E = 2$  Kev and  $t = 20$  Kev, then at an incident proton energy around 1 Mev on a target of  $Z \sim 12$ , the straggling effect would be that shown by the broken line in Fig. 10 (H.E. Gove, 1959).

It can be seen, then, from the above arguments, that in order to get a step height in the experimental yield curve to within a few percent of  $Y(\infty)$ , then certain conditions have to be met. These conditions are that  $t > 40\Gamma$  or  $> 4\Delta E b$  whichever is the greater, and providing these conditions are met then effects on the step height of the yield curve due to straggling will not be appreciable in the proton energy

range used. The condition that  $t > 4\Delta E b$  must be held to rigidly as the corrections involved if this is not true are very complex. However, if the other condition is not obeyed for some reason then the corrections involved are quite straight-forward.

The targets described up to now are known as 'thick' targets for the obvious reason that  $t \gg \Gamma$ . In certain circumstances 'thin' targets, i.e.  $t \ll \Gamma$ , can be used to obtain a yield curve, and it can easily be shown that the area under a yield curve from a thin target will be, (H.E. Gove, 1959):-

$$= n \int_0^{\infty} \sigma(E) dE$$

where  $n$  is the target thickness in atoms/cm<sup>2</sup>.

Obviously, if  $\Delta E b \ll t$  and  $t \ll \Gamma$ , then the yield curve obtained would take on the Breit-Wigner shape of FWHM =  $\Gamma$ . If, however,  $\Delta E b \sim \Gamma$  then the yield curve shape and area under the yield curve from the thin target would differ greatly from that predicted by theory. As  $\Delta E b$  of the Van de Graaff used was  $\sim 1$  Kev, and the largest  $\Gamma$  studied was  $\sim 5$  Kev, it was decided to use 'thick' targets in all the cases studied.

Therefore, for a thick target, it is known that:-

$$\begin{aligned} y(\infty) &= \pi/2 \cdot 1/k \cdot \sigma_R \Gamma \\ &= \frac{2\pi^2}{k} \cdot \lambda^2 \frac{(2J_1 + 1)}{(2i_1 + 1)(2I_0 + 1)} \frac{\Gamma_p \Gamma_\gamma}{\Gamma} \end{aligned}$$

Providing then, that  $Y(\infty)$  can be measured, and  $k$  and  $\Gamma_p/\Gamma$  known,  $\Gamma_\gamma$  can be found by the techniques described above.

However, with targets made by evaporation techniques, it cannot always be assumed that the constituency of the target material is the same before and after evaporation. Because of this, it is more reliable to use a method for finding  $\Gamma_\gamma$  that involves knowing relative  $k$ -values instead of absolute values. In order to use this technique, an absolute value of resonance strength for one of the resonances under study must be known. The value of  $\omega_\gamma$  for the 511 Kev resonance in  ${}_{11}\text{Na}^{23}(p,\gamma){}_{12}\text{Mg}^{24}$  has been found quite accurately by Enkelbertink (1966) involving a standard  $\omega_\gamma$  known from a resonant absorption experiment. Enkelbertink had used, among others, a NaCl target and had found that the constituency of NaCl had not changed appreciably after evaporation. It was, therefore, proposed to use 'thick' NaCl targets for finding the  $\Gamma_\gamma$ 's of various resonances and to use the  $\omega_\gamma$  of the 511 Kev resonance as the standard resonance strength.

For a relative calculation involving two resonances it can be written then that:-

$$\frac{Y_1(\infty)}{Y_2(\infty)} = \frac{\chi_1^2}{\chi_2^2} \cdot \frac{k_2}{k_1} \cdot \frac{(2J_1 + 1)}{(2J_2 + 1)} \cdot \frac{\Gamma_{p1}}{\Gamma_1} \cdot \frac{\Gamma_2}{\Gamma_{p2}} \cdot \frac{\Gamma_{\gamma 1}}{\Gamma_{\gamma 2}}$$

The values of  $(k_2/k_1)$  were found from extensive

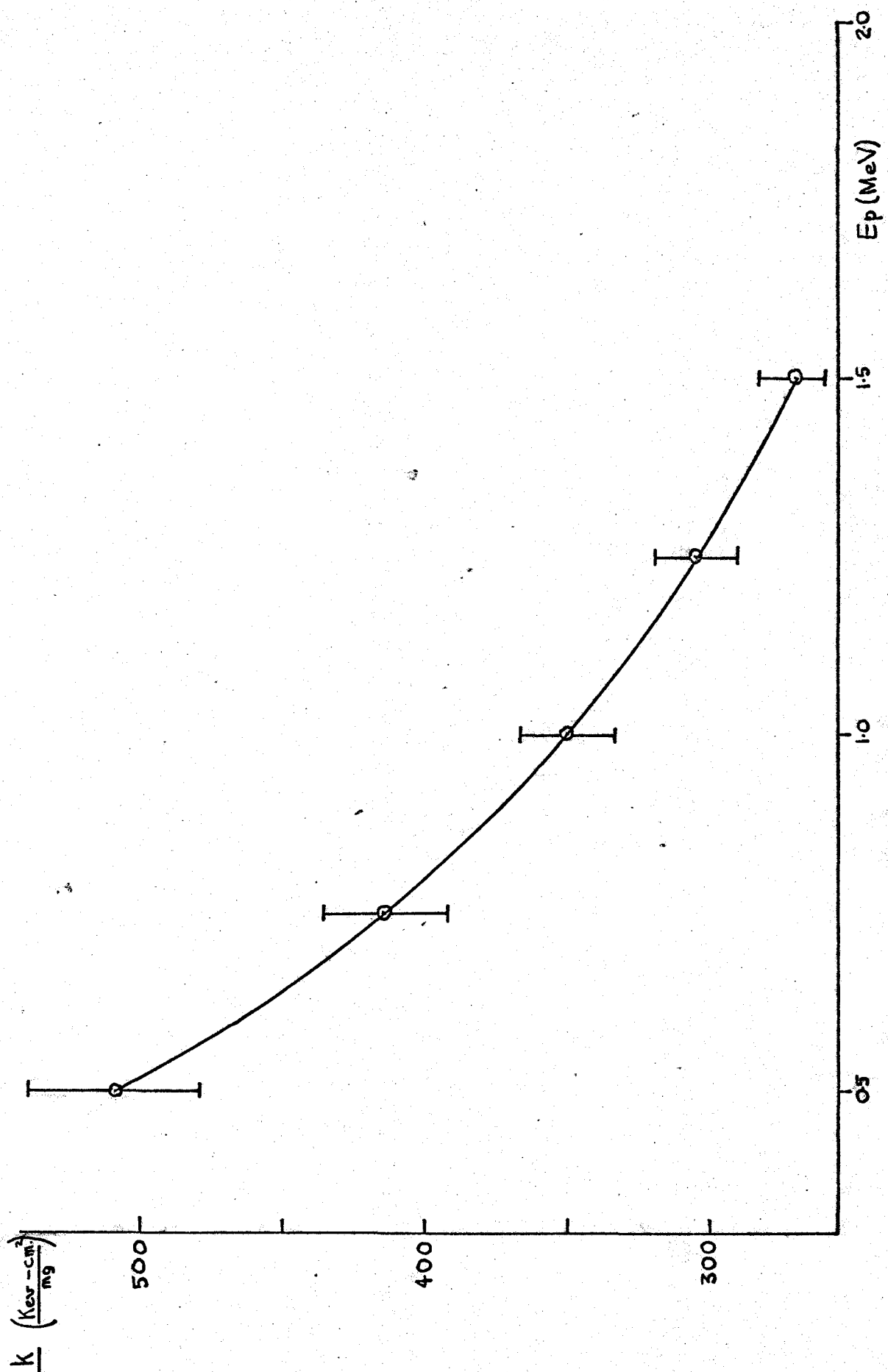


FIG. 11. ATOMIC STOPPING CROSS SECTION FOR Na IN NaCl.

work on stopping powers done by Whaling (1958). A graph of the relative stopping powers used is shown in Fig. 11.

(ii) Measurement of  $Y(\infty)$ .

The value of  $Y(\infty)$  for a particular resonance may be found by counting the number of primary gamma rays coming from the resonance concerned, for a certain incident proton number. With the technique explained previously, however, we are only interested in relative values of  $Y(\infty)$  for any two resonances. These measurements were carried out by recording a Ge(Li) spectrum at  $55^\circ$  for both resonances concerned. The same target was used for studying both resonances in order to ensure that the target was the same constituency for both resonances, and, therefore, the relative stopping powers used would, most likely, be correct. In order to avoid excessive deterioration of the target during the runs on the two resonances, only low proton currents, e.g.  $\sim 2-3$  microamps, were used, and the runs were of only sufficient duration so as to give about 5% statistical error in the area of the most intense primary gamma ray peak in the spectrum, from the resonance concerned.

Once the areas under the above peaks were known, the appropriate efficiency corrections were applied in order to find the relative  $A_0$  value for those particular gamma rays. It was not necessary to take into account angular distribution effects, due to the size of the statistical

errors involved. Knowing the relative  $A_0$  value and the branching ratios of the particular decays from the previous work done in this thesis, then the ratio of the total number of primary gamma rays from each resonance can be found by obvious means.

Of course, the runs on the two resonances concerned must also be normalized to unit incident proton number. This was achieved by measuring the total integrated current, i.e. total charge, collected on the target during the run on each resonance, and then normalizing each run to unit incident charge.

We have then that the ratio of the  $Y(\infty)$  values for two resonances is given in the formula:-

$$\frac{Y_1(\infty)}{Y_2(\infty)} = \frac{A_1}{A_2} \cdot \frac{\epsilon_2}{\epsilon_1} \cdot \frac{B_2}{B_1} \cdot \frac{N_2}{N_1}$$

where:-  $A_1$  = area under peak concerned in resonance 1.

$A_2$  = area under peak concerned in resonance 2.

$\epsilon_1$  = relative efficiency of gamma ray from resonance 1.

$\epsilon_2$  = relative efficiency of gamma ray from resonance 2.

$B_1$  = branching ratio of gamma ray from resonance 1.

$B_2$  = branching ratio of gamma ray from resonance 2.

$N_1$  = charge collected during run on resonance 1.

$N_2$  = charge collected during run on resonance 2.

The above formula assumes, of course, that the target used in the study of the two resonances, obeys the conditions for a 'thick' target. If these conditions are not met with, then the correction explained previously must be applied to the final result.

It should be pointed out that in order to get a true reading of the charge collected on the target during a run, it was necessary to suppress secondary emission of electrons from the target by putting a voltage, negative with respect to the target, on the tantalum beam stop mentioned previously. It was found that 100 volts on the beam stop was enough to suppress secondary emission over the range of proton energies used in this experiment.

## CHAPTER 3

### EXPERIMENTAL RESULTS

#### 3.1 Introduction

This chapter contains the experimental results obtained for six resonances in  $\text{Na}^{23}(\text{p},\gamma)\text{Mg}^{24}$ . These are  $E_p = 512$  Kev, 987 Kev, 1020 Kev, 1174 Kev, 1318 Kev and 1416 Kev. These resonances were studied because of their relatively large gamma ray yields, because very little of the  $\text{Na}^{23}(\text{p},\text{p}'\gamma)\text{Na}^{23}$  and  $\text{Na}^{23}(\text{p},\alpha)\text{Ne}^{20}$  reactions occur at these resonances, and because  $\Gamma_p \gg \Gamma_\gamma$  (Nordhagen, 1964). This ensures that  $\Gamma_p/\Gamma$  can be approximated to unity in the gamma transition width calculations, except in the 1416 Kev resonance where  $\Gamma_p/\Gamma = 0.5$ .

The decay schemes and branching ratios were found for each resonance. Also the gamma transition width for each resonance, except the 1416 Kev, was found and the partial gamma widths for the gamma decays from the resonance were compared to Single Particle Estimates.

#### 3.2 Results

(i)  $E_p = 512$  Kev Resonance.

This resonance was studied with a NaCl target about 10 Kev thick at the resonance energy. Gamma ray spectra were

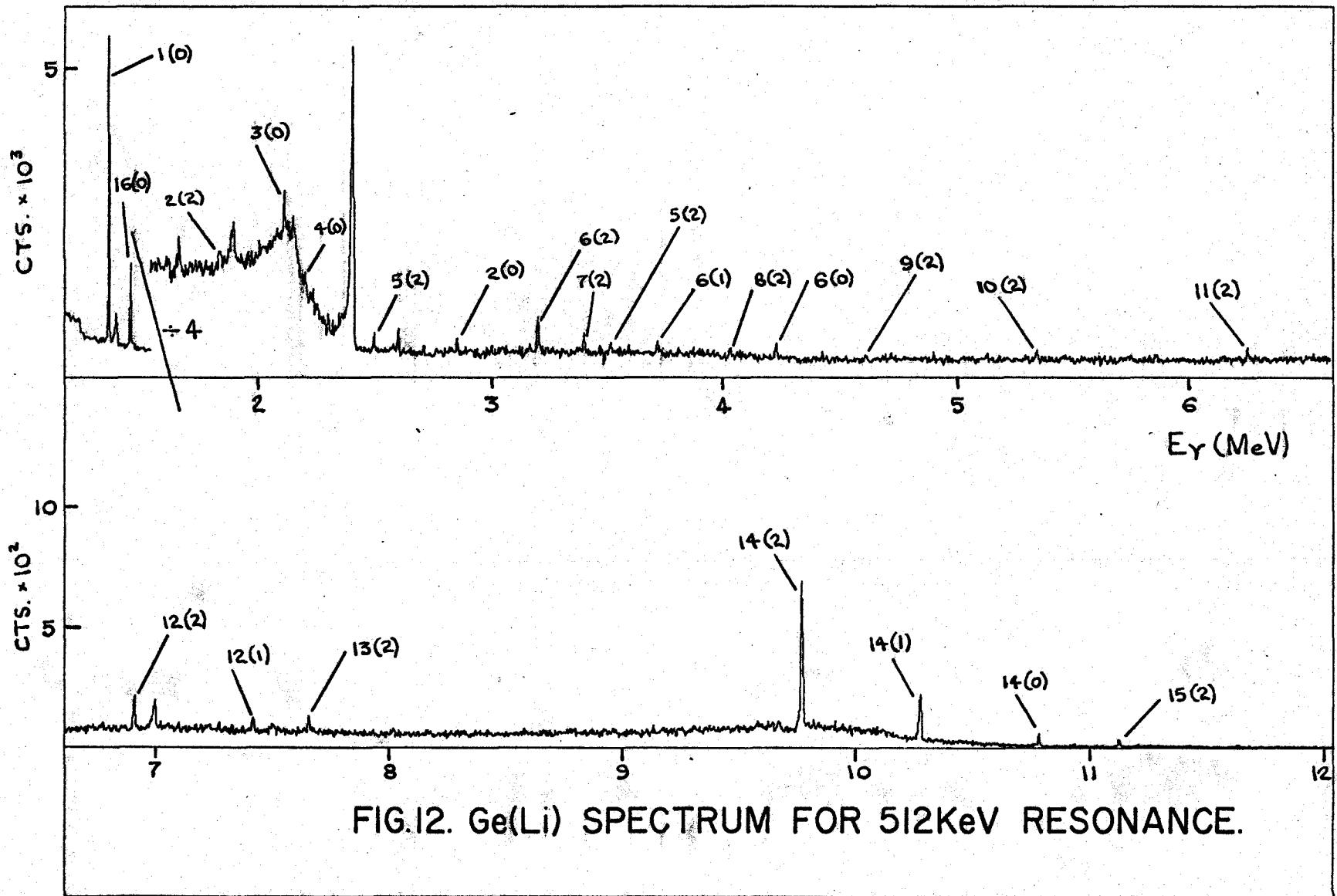


FIG.12. Ge(Li) SPECTRUM FOR 512KeV RESONANCE.

<u>Transition Number</u>	<u>Transition</u>
1	1.37 Mev $\rightarrow$ g.s.
2	4.24 Mev $\rightarrow$ 1.37 Mev
3	Res. $\rightarrow$ 10.07 Mev
4	Res. $\rightarrow$ 9.98 Mev
5	Res. $\rightarrow$ 8.65 Mev
6	4.24 Mev $\rightarrow$ g.s.
7	Res. $\rightarrow$ 7.75 Mev
8	6.44 Mev $\rightarrow$ 1.37 Mev
9	Res. $\rightarrow$ 6.44 Mev
10	7.75 Mev $\rightarrow$ 1.37 Mev
11	8.65 Mev $\rightarrow$ 1.37 Mev
12	Res. $\rightarrow$ 4.24 Mev
13	10.07 Mev $\rightarrow$ 1.37 Mev
14	Res. $\rightarrow$ 1.37 Mev
15	Res. $\rightarrow$ g.s.
16	$E_{\gamma} = 1.46$ Mev from $K^{40}$ background

TABLE 3: Identification of the peaks in the Ge(Li) Spectrum for the 512 Kev Resonance.

obtained with the Ge(Li) counter at  $0^\circ$ ,  $55^\circ$  and  $90^\circ$ . The  $55^\circ$  spectrum is shown in Fig. 12. This represents a run of about 6.5 hours with a proton current of about 10 microamps. Each peak in the spectrum is numbered and the explanation of these numbers is given in Table 3. The figures in brackets correspond to whether the peak is a 2nd escape, i.e. (2), 1st escape, i.e. (1), or a full energy, i.e. (0).

The decay scheme was found from the  $90^\circ$  run as previously explained. The very accurately known energy of the 1.37 Mev gamma ray in this spectrum was used as the reference, together with the 511 Kev full energy, 1st and 2nd escape peak energy differences, as explained in a previous section. The energy dispersion in this spectrum was extremely linear up to about 8 Mev and permitted a very accurate calculation of the energies of the gamma rays concerned. Most of these energies are much more accurate than have previously been obtained from NaI detectors.

For the branching ratio work the  $0^\circ$ ,  $55^\circ$ , and  $90^\circ$  spectra were initially normalized by using the "greater than 2 Mev" gate readings, but these were found to be inaccurate due to the deterioration of the target during the runs. However, a normalization was achieved using the fixed angle, NaI spectrum technique with much shorter runs on the Ge(Li) counter at the same angles as before. The initial runs were then normalized to the shorter runs using the most intense transition, the Res.  $\rightarrow$  1.37 Mev, in the spectrum.

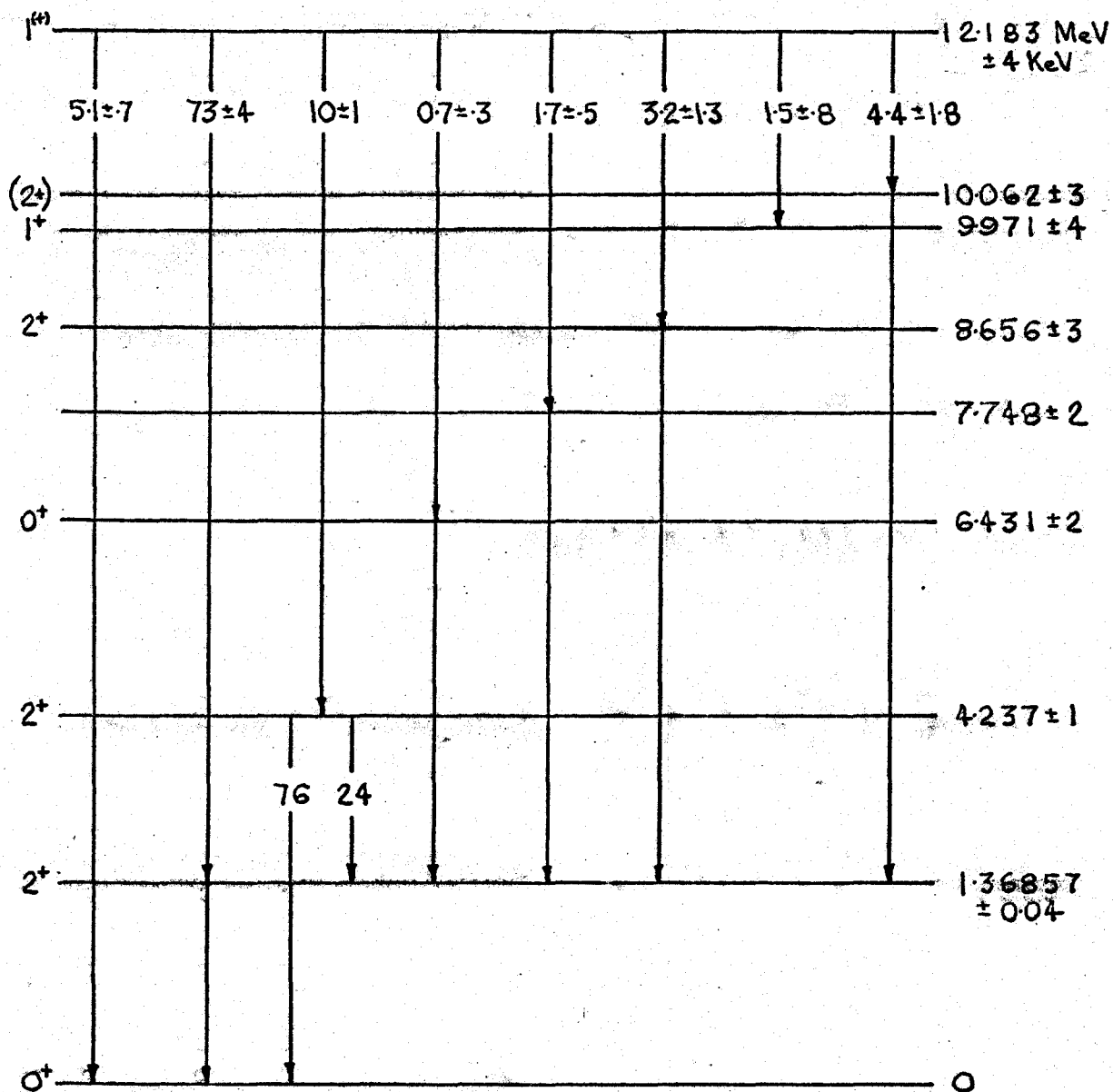


FIG.13. DECAY SCHEME FOR 512KeV RESONANCE.

This technique was successful but obviously introduced larger errors than would have resulted from a direct normalization.

The angular distribution found for the  $R \rightarrow 1.37$  Mev transition was almost isotropic and contained no  $P_4(\cos \theta)$  term, within the errors of the results. For this reason the  $A_0$  value for this transition was found from the  $55^\circ$  run only, where  $P_2(\cos \theta) = 0$ . The  $A_0$  values of all the other transitions were also found from the  $55^\circ$  run only, since the magnitude of the statistical errors involved did not warrant a correction for a possible  $P_4(\cos \theta)$  term in the angular distribution.

The decay scheme, together with branching ratios is shown in Fig. 13. This scheme compares almost exactly with that given in Endt and Van der Leun (1962), except that some of the secondary gamma rays were not seen in this experiment due to the inadequate statistics.

As has been mentioned previously, the gamma transition width for this resonance has been taken from work by Engelbertink (1966), who found  $\Gamma_\gamma = 0.35 (\pm 0.056)$  ev. From this value of  $\Gamma_\gamma$ , and from the branching ratios found in this experiment, the partial gamma ray widths of the transitions from the resonance were found. These partial widths were then compared to Single Particle Estimates for the transitions concerned, and the partial reduced transition

<u>Transition</u>	$\frac{\Gamma_{\text{exp}}}{\Gamma(\text{E1})}$	$\frac{\Gamma_{\text{exp}}}{\Gamma(\text{M1})}$	$\frac{\Gamma_{\text{exp}}}{\Gamma(\text{E2})}$
Res. $\rightarrow$ 1.37 Mev	$3.5 \times 10^{-4}$	$1.0 \times 10^{-2}$	
Res. $\rightarrow$ 4.24 Mev	$1.2 \times 10^{-4}$	$3.6 \times 10^{-3}$	
Res. $\rightarrow$ g.s.	$1.7 \times 10^{-5}$	$5.0 \times 10^{-4}$	$1.9 \times 10^{-1}$
Res. $\rightarrow$ 10.06 Mev	$2.7 \times 10^{-3}$	$7.9 \times 10^{-2}$	
Res. $\rightarrow$ 8.66 Mev	$4.3 \times 10^{-4}$	$1.3 \times 10^{-2}$	
Res. $\rightarrow$ 7.75 Mev	$1.2 \times 10^{-4}$	$3.4 \times 10^{-3}$	
Res. $\rightarrow$ 6.43 Mev	$2.3 \times 10^{-5}$	$6.6 \times 10^{-4}$	$1.1 \times 10^{-1}$
Res. $\rightarrow$ 9.97 Mev	$8.3 \times 10^{-4}$	$2.4 \times 10^{-2}$	

TABLE 4: Comparison to Single Particle Estimates in the 512 Kev Resonance.

strengths found are shown in Table 4. It can be seen from this table that the reduced transition strengths are smaller, by about an order of magnitude, than those values for similar transitions for the other resonances reported in this thesis. The reduced strengths for the Res.  $\rightarrow$  g.s. and Res.  $\rightarrow$  6.43 Mev transitions, which must be pure multipoles, are even smaller. In fact, from the reduced strengths for these two transitions, one might be tempted to suggest that a spin of  $2^+$  for this resonance would be more acceptable. In this connection, it is interesting to note that the angular correlation measurements made by Glaudemans and Endt (1962) are consistent with a resonance spin of  $1^+$ ,  $1^-$  or  $2^+$ , but spin 1 was more probable.

Although a spin  $2^+$  assignment seems possible, the smallness of the comparison values is most probably due to the nuclear matrix elements of this resonance being much different from those of the other resonances studied.

If the resonance is in fact spin 1 then the comparison values for the E1 and M1 transitions, shown in Table 4, give no indication as to whether the resonance spin is  $1^+$  or  $1^-$ .

(ii)  $E_p = 987$  Kev Resonance.

This resonance was studied with a NaOH target of about 5 Kev thickness at  $E_p \sim 1$  Mev. Gamma ray spectra using the Ge(Li) counter were obtained at  $0^\circ$ ,  $55^\circ$  and  $90^\circ$ . The  $55^\circ$

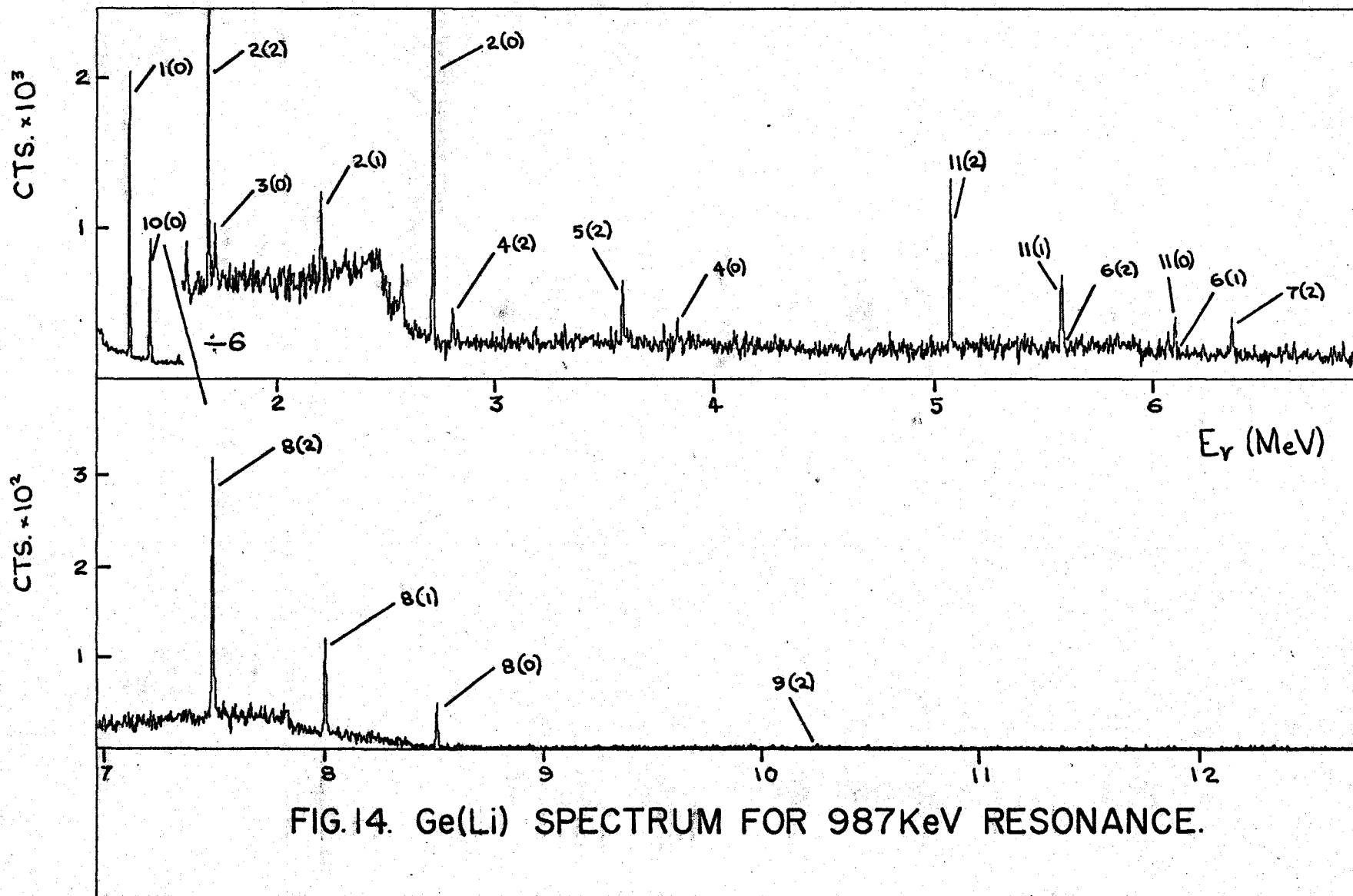


FIG.14. Ge(Li) SPECTRUM FOR 987KeV RESONANCE.

<u>Transition Number</u>	<u>Transition</u>
1	1.37 Mev $\rightarrow$ g.s.
2	4.12 Mev $\rightarrow$ 1.37 Mev
3	6.00 Mev $\rightarrow$ 4.24 Mev
4	5.23 Mev $\rightarrow$ 1.37 Mev
5	6.00 Mev $\rightarrow$ 1.37 Mev
6*	Res. $\rightarrow$ 6.00 Mev
7	Res. $\rightarrow$ 5.23 Mev
8	Res. $\rightarrow$ 4.12 Mev
9	Res. $\rightarrow$ 1.37 Mev
10	$E_{\gamma} = 1.46$ Mev from $K^{40}$ background
11	$E_{\gamma} = 6.13$ Mev from $F^{18}$ (p, $\alpha$ ) $O^{16}$ background

\* This transition is hidden at the bases of the large background peaks.

TABLE 5: Identification of the peaks in the Ge(Li) Spectrum for the 987 KeV Resonance.

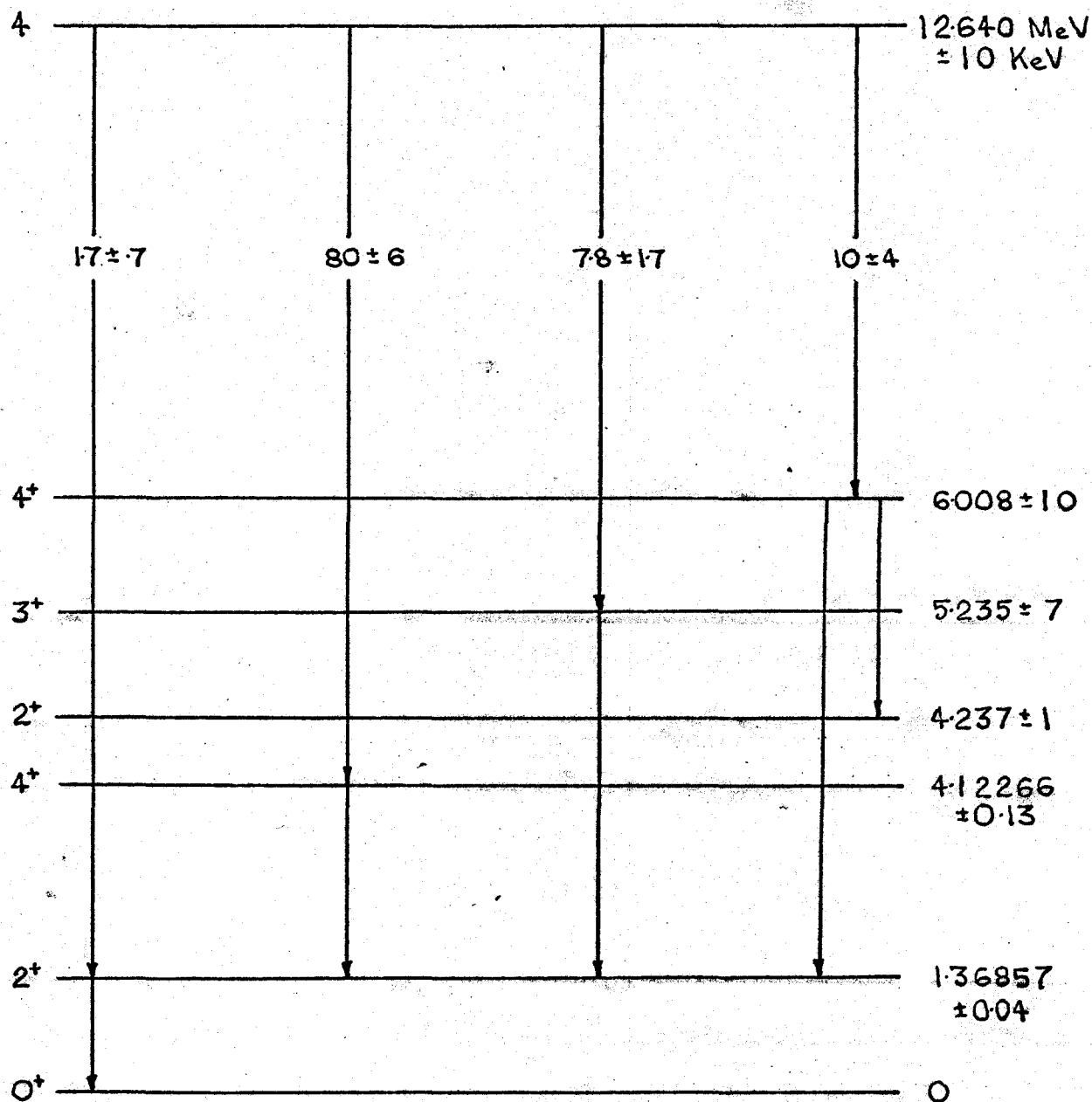


FIG. 15. DECAY SCHEME FOR 987 KeV RESONANCE.

run is shown in Fig. 14 and the identification of the peaks is explained in Table 5. This represents a run of about 3 hours duration using a proton current of around 2.5 microamps.

The decay scheme was found from the  $90^\circ$  run using the very accurately known energies of the 1.37 Mev and 2.75 Mev gamma rays as standards.

The branching ratios were obtained using only the  $55^\circ$  run since, again, the statistics of the experiment did not warrant making a correction for a  $P_4(\cos \theta)$  term.

The decay scheme, together with branching ratios is shown in Fig. 15. This scheme compares very well with that shown in Endt and Van der Leun (1967), except that no Res.  $\rightarrow$  4.24 Mev transition was seen in the present work. This confirms work done by Nordhagen (1964), who also saw no Res.  $\rightarrow$  4.24 Mev transition but who, however, did not see the Res.  $\rightarrow$  5.23 Mev transition that is definitely present.

The gamma transition width of this resonance was found by comparing its gamma ray yield directly with that of the 511 Kev resonance in the manner explained previously. A NaCl target of about 14 Kev thickness at  $E_p \sim 1$  Mev was used for the comparison experiment.

The most intense transition from each resonance was used in the calculations. It was found that for this resonance  $\Gamma_\gamma = 0.33 (\pm 0.13)$  ev. From this figure and the branching ratios found in this experiment, the partial gamma ray

<u>Transition</u>	$\frac{\Gamma_{\text{exp}}}{\Gamma(\text{E1})}$	$\frac{\Gamma_{\text{exp}}}{\Gamma(\text{M1})}$	$\frac{\Gamma_{\text{exp}}}{\Gamma(\text{E2})}$	$\frac{\Gamma_{\text{exp}}}{\Gamma(\text{M2})}$
Res. $\rightarrow$ 4.12	$7.2 \times 10^{-4}$	$2.1 \times 10^{-2}$		
Res. $\rightarrow$ 6.00	$2.1 \times 10^{-4}$	$6.0 \times 10^{-3}$		
Res. $\rightarrow$ 5.23	$1.1 \times 10^{-4}$	$3.2 \times 10^{-3}$		
Res. $\rightarrow$ 1.37			$8.9 \times 10^{-3}$	$3.7 \times 10^{-1}$

TABLE 6: Comparison to Single Particle Estimates in the 987 Kev Resonance.

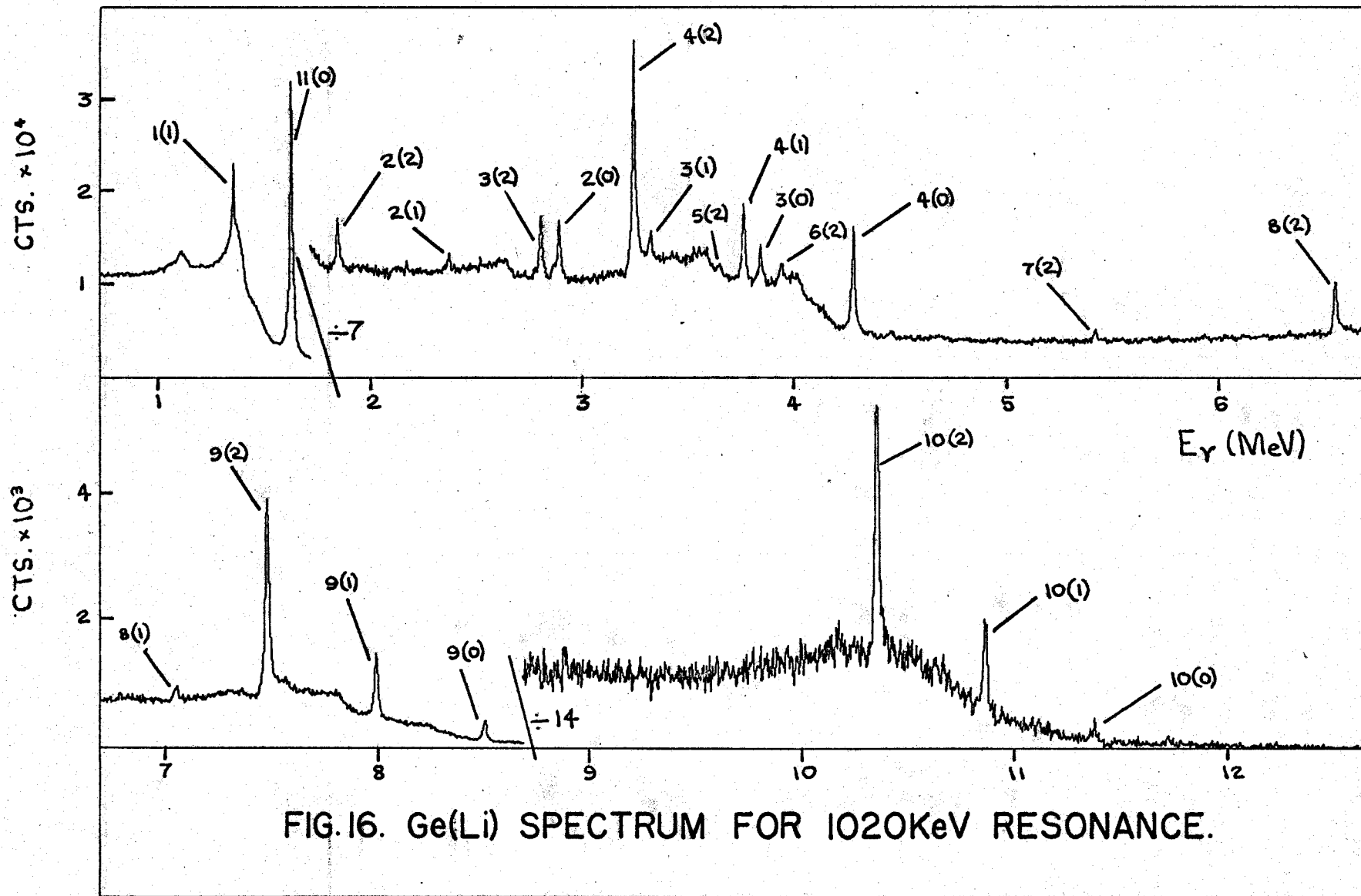


FIG.16. Ge(Li) SPECTRUM FOR 1020KeV RESONANCE.

<u>Transition Number</u>	<u>Transition</u>
1	1.37 Mev $\rightarrow$ g.s.
2	4.24 Mev $\rightarrow$ 1.37 Mev
3	Res. $\rightarrow$ 8.87 Mev
4	4.24 Mev $\rightarrow$ g.s.
5	8.87 Mev $\rightarrow$ 4.24 Mev
6	Res. $\rightarrow$ 7.75 Mev
7	7.75 Mev $\rightarrow$ 1.37 Mev
8	8.87 Mev $\rightarrow$ 1.37 Mev
9	Res. $\rightarrow$ 4.24 Mev
10	Res. $\rightarrow$ 1.37 Mev
11	$E_{\gamma} = 1.63$ Mev from $\text{Na}^{23}$ (p, $\alpha$ ) $\text{Ne}^{20}$ reaction

TABLE 7: Identification of the peaks in the Ge(Li) Spectrum for the 1020 Kev Resonance.

widths of the transitions from the resonance were found and compared to Single Particle Estimates. These partial reduced transition strengths are shown in Table 6. It can be seen that the values in this table give no indication whether the spin of the resonance is  $4^+$  or  $4^-$ .

(iii)  $E_p = 1020$  Kev Resonance.

As the natural width of this resonance is around 4 Kev, a target of NaCl of around 20 Kev thickness at  $E_p \sim 1$  Mev was used in the study of this resonance. This target gives, therefore, almost the maximum possible gamma ray yield from the resonance in question without including any nearby large resonances. A short run was carried out, at  $90^\circ$ , at an energy about 10 Kev below the 1020 Kev resonance, where a smaller resonance was present. From this run it was concluded that the gamma rays from this lower resonance could not be confused with those from the 1020 Kev resonance.

Gamma ray spectra from the Ge(Li) counter were obtained at  $0^\circ$ ,  $35^\circ$ ,  $55^\circ$ ,  $75^\circ$  and  $90^\circ$ . The  $55^\circ$  run is shown in Fig. 16, and the identification of the peaks explained in Table 7. This represents a run of about 2.25 hours duration at a proton current of around 20 microamps.

The decay scheme was found from the  $90^\circ$  run using the 1.37 Mev and 4.24 Mev gamma rays as standards. The value of the 4.24 Mev gamma ray was found accurately from the analysis of the 511 Kev resonance.

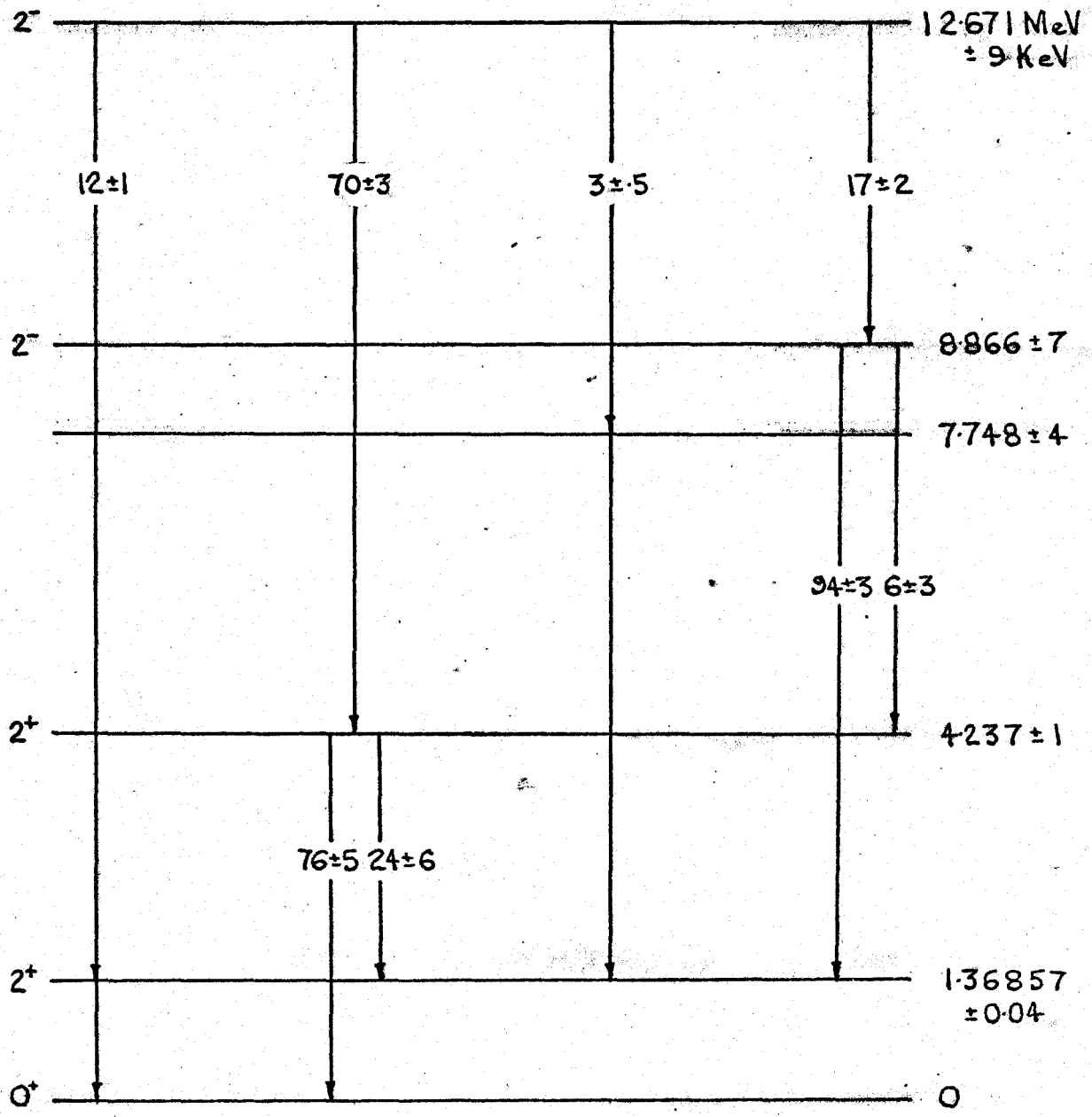


FIG. 17. DECAY SCHEME FOR 1020KeV RESONANCE.

For the branching ratio work the runs were normalized using the fixed angle NaI technique. The  $A_0$  value of the Res.  $\rightarrow$  4.24 Mev was found from the angular distribution of the gamma rays concerned at all angles measured. The angular distribution for this gamma was found to be  $W(\theta) \propto 1 - 0.141 (\pm 0.03)P_2(\cos \theta) + 0.051 (\pm 0.031)P_4(\cos \theta)$ . The  $A_0$  value for the Res.  $\rightarrow$  8.87 Mev transition was found, in a similar way, to be  $W(\theta) \propto 1 - 0.147 (\pm 0.06)P_2(\cos \theta) + 0.027 (\pm 0.08)P_4(\cos \theta)$ . The  $A_0$  values for all the other decays were found from the  $55^\circ$  run only, due to the statistics of the experiment.

The decay scheme found, together with the branching ratios, is shown in Fig. 17. The most important feature of this decay scheme is the reassignment of the previously thought Res.  $\rightarrow$  5.23 Mev  $\rightarrow$  1.37 Mev cascade, to the Res.  $\rightarrow$  8.87 Mev  $\rightarrow$  1.37 Mev cascade. The primary and secondary of this cascade had previously been confused due to the poor resolution of NaI detectors. Also, a weak 8.87 Mev  $\rightarrow$  4.24 Mev transition was seen that had not been reported previously. From branching ratio work, the Res.  $\rightarrow$  7.75 Mev  $\rightarrow$  1.37 Mev cascade was found to be a 100% cascade to within 20%.

Apart from the above cases the decay scheme agreed with that shown in Endt and Van der Leun (1967), although some of the weaker secondaries were not seen due to the statistics of the experiment.

<u>Transition</u>	$\frac{\Gamma_{\text{exp}}}{\Gamma(\text{E1})}$	$\frac{\Gamma_{\text{exp}}}{\Gamma(\text{M1})}$	$\frac{\Gamma_{\text{exp}}}{\Gamma(\text{E2})}$
Res. $\rightarrow$ 4.24 Mev	$7.5 \times 10^{-3}$		
Res. $\rightarrow$ 8.87 Mev		$5.7 \times 10^{-1}$	
Res. $\rightarrow$ 1.37 Mev	$5.4 \times 10^{-4}$		
Res. $\rightarrow$ 7.75 Mev	$1.5 \times 10^{-3}$	$4.2 \times 10^{-2}$	$1.0 \times 10^{-1}$

TABLE 8: Comparison to Single Particle Estimates for the 1020 KeV Resonance.

The gamma transition width of this resonance was found by comparing its gamma ray yield to that of the 987 Kev resonance. A NaCl target of about 25 Kev thickness at  $E_p \sim 1$  Mev was used in the comparison experiment. This ensured that the step in the thick target yield curve of the 1020 Kev resonance would be within 10% of  $Y(\infty)$  for that resonance. As might be expected, the gamma ray yield from the 987 Kev resonance, using the above target, was found to be the same, within statistical errors, as that from the 987 Kev resonance using the target previously used for finding the gamma transition width of the 987 Kev resonance. This meant that the gamma ray yield from the 1020 Kev resonance could be compared directly to that from the 512 Kev resonance. The most intense transition in each resonance was used in the calculation.

It was found that for this resonance  $\Gamma_\gamma = 3.79$  ( $\pm 0.8$ ) ev. From this figure and the branching ratios found in this experiment, the partial gamma ray widths of the transition from the resonance were found and compared to Single Particle Estimates. These reduced transition strengths are shown in Table 8.

It should be pointed out that the spin and parity of the 8.87 Mev level has been found very recently, (Mabey, 1968), to be  $2^-$ . The angular distribution and the partial reduced gamma width for the Res.  $\rightarrow$  8.87 Mev show nothing to

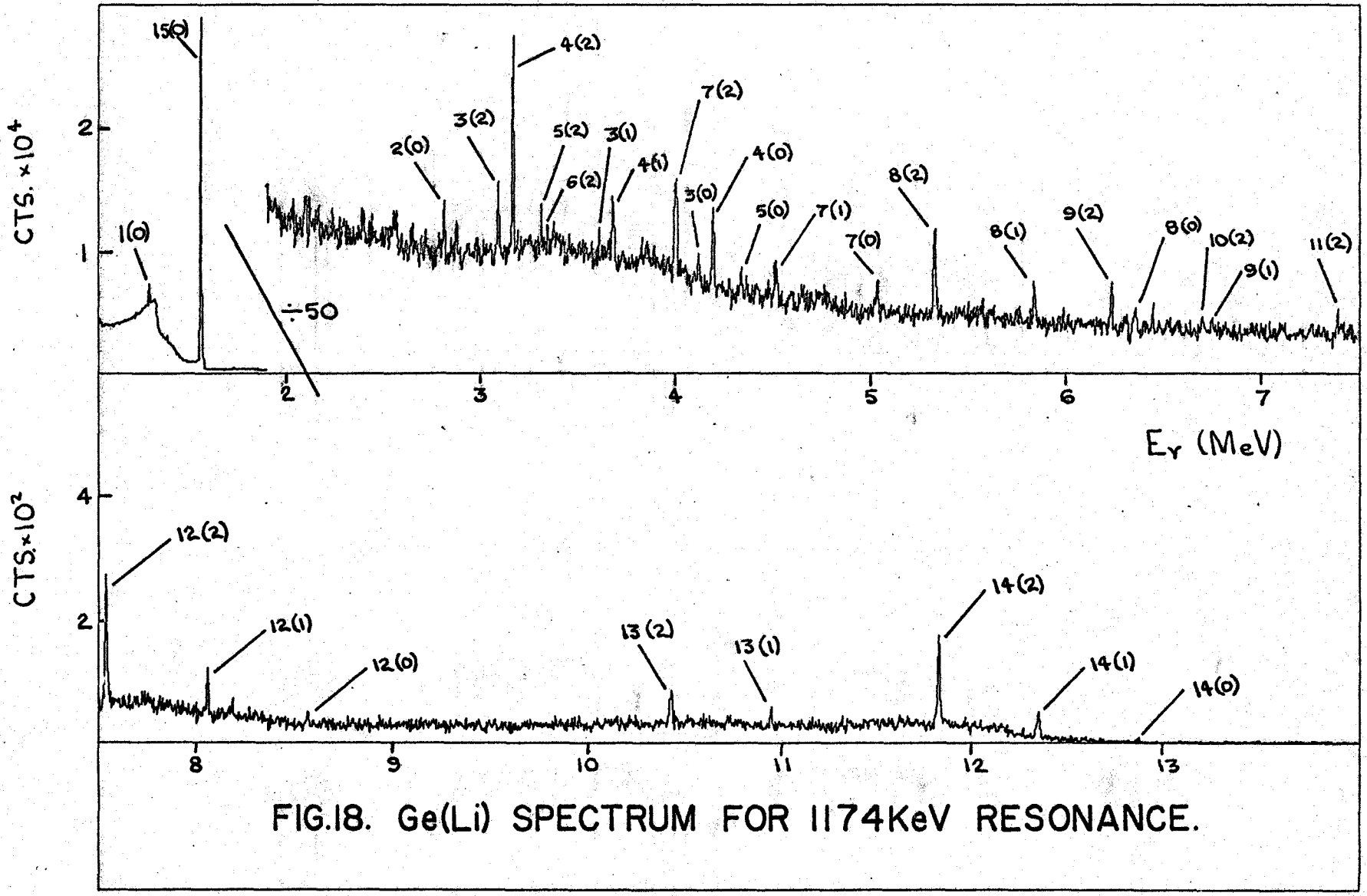


FIG.18. Ge(Li) SPECTRUM FOR 1174KeV RESONANCE.

<u>Transition Number</u>	<u>Transition</u>
1	1.37 Mev $\rightarrow$ g.s.
2	4.24 Mev $\rightarrow$ 1.37 Mev
3	Res. $\rightarrow$ 8.65 Mev
4	4.24 Mev $\rightarrow$ g.s.
5	Res. $\rightarrow$ 8.44 Mev
6	8.65 Mev $\rightarrow$ 4.24 Mev
7	$E_{\gamma} = 5.07$ Mev
8	$E_{\gamma} = 6.38$ Mev
9	8.65 Mev $\rightarrow$ 1.37 Mev
10	7.75 Mev $\rightarrow$ g.s.
11	8.44 Mev $\rightarrow$ g.s.
12	Res. $\rightarrow$ 4.24 Mev
13	Res. $\rightarrow$ 1.37 Mev
14	Res. $\rightarrow$ g.s.
15	$E_{\gamma} = 1.63$ Mev from $\text{Na}^{23}$ (p, $\alpha$ ) $\text{Ne}^{20}$ reaction

TABLE 9: Identification of the peaks in the Ge(Li) Spectrum for the 1174 Kev Resonance.

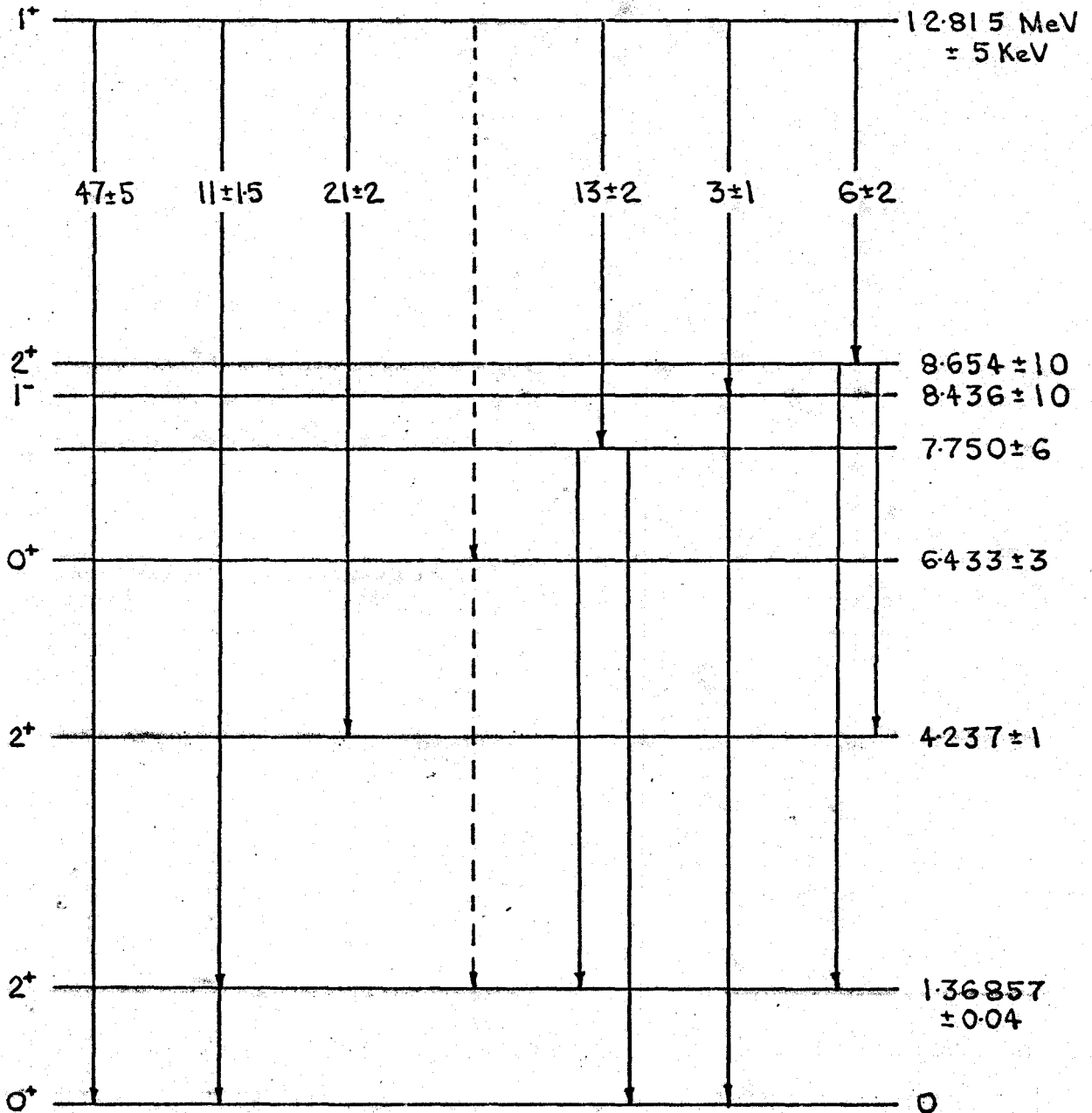


FIG.19. DECAY SCHEME FOR 1174KeV RESONANCE.

doubt this assignment.

(iv)  $E_p = 1174$  Kev Resonance.

A NaCl target of about 5 Kev thickness at  $E_p \sim 1$  Mev was used to investigate this resonance. With a target of this thickness the contribution from the 1163 Kev resonance should be negligible.

Gamma ray spectra from the Ge(Li) counter were obtained at  $0^\circ$ ,  $55^\circ$ , and  $90^\circ$ . The  $55^\circ$  run is shown in Fig. 18 and the identification of the peaks is explained in Table 9. This represents a run of about 2 hours duration at a proton current of around 5 microamps.

The decay scheme was found in a similar way to that for the 1020 Kev resonance.

For the branching ratio work, the  $A_0$  values for all the transitions were found from the  $55^\circ$  run.

The decay scheme, together with branching ratios, is shown in Fig. 19. The improvement of this decay scheme over what was previously found is a prime example of the advantage of using Ge(Li) detectors.

Firstly, the cascade of the Res.  $\rightarrow 5.23$  Mev  $\rightarrow 1.37$  Mev had previously been confused with the Res.  $\rightarrow 8.65$  Mev  $\rightarrow 1.37$  Mev cascade and partly with the Res.  $\rightarrow 8.44 \rightarrow$  g.s. cascade.

Secondly, the Res.  $\rightarrow 7.75$  Mev  $\rightarrow 1.37$  Mev cascade requires exactly the same gamma ray energies as the Res.  $\rightarrow 6.44$

Mev  $\rightarrow$  1.37 Mev cascade, namely, 6.38 Mev and 5.07 Mev. Some confusion arises here as to whether one, or the other, or both cascades are present. The existence of a 7.75 Mev  $\rightarrow$  g.s. transition indicates that at least the Res.  $\rightarrow$  7.75 Mev transition is taking place. No 6.44 Mev  $\rightarrow$  4.24 Mev transition is seen but this is not unreasonable considering the statistics of the experiment. This anomaly could not be cleared up by observing the Doppler shift of the gamma rays at  $0^\circ$ , as the energies of both gamma rays were shifted by approximately equal proportions.

The  $A_0$  values, corrected for efficiency, for the 6.38 Mev, 5.07 Mev and 7.75 Mev gamma rays are shown below:-

<u>Gamma Energy (Mev)</u>	<u><math>A_0</math></u>
5.07	174 ( $\pm 24$ )
6.38	168 ( $\pm 23$ )
7.75	23 ( $\pm 8$ )

It can be seen from these figures and from the branching ratios found at the 1020 Kev resonance, that most of the above gamma rays are involved in the Res.  $\rightarrow$  7.75 Mev  $\rightarrow$  1.37 Mev cascade but the possibility of the Res.  $\rightarrow$  6.44 Mev  $\rightarrow$  1.37 Mev cascade cannot be excluded.

The gamma transition width for this resonance was found in an exactly similar way and with the same target as that for the 1020 Kev resonance. The only difference was that the Res.  $\rightarrow$  4.24 Mev transition of the 1174 Kev resonance was

<u>Transition</u>	$\frac{\Gamma_{\text{exp}}}{\Gamma(E1)}$	$\frac{\Gamma_{\text{exp}}}{\Gamma(M1)}$	$\frac{\Gamma_{\text{exp}}}{\Gamma(E2)}$
Res. $\rightarrow$ g.s.		$5.2 \times 10^{-2}$	
Res. $\rightarrow$ 4.24 Mev		$7.8 \times 10^{-2}$	
Res. $\rightarrow$ 1.37 Mev		$1.7 \times 10^{-2}$	
Res. $\rightarrow$ 8.65 Mev		$1.9 \times 10^{-1}$	
Res. $\rightarrow$ 8.44 Mev	$2.8 \times 10^{-3}$		
If Res. $\rightarrow$ 7.75 Mev	$7.8 \times 10^{-3}$	$2.3 \times 10^{-1}$	$5 \times 10^{-1}$
If Res. $\rightarrow$ 6.44 Mev		$1.2 \times 10^{-1}$	

TABLE 10: Comparison to Single Particle Estimates for the 1174 Key Resonance.

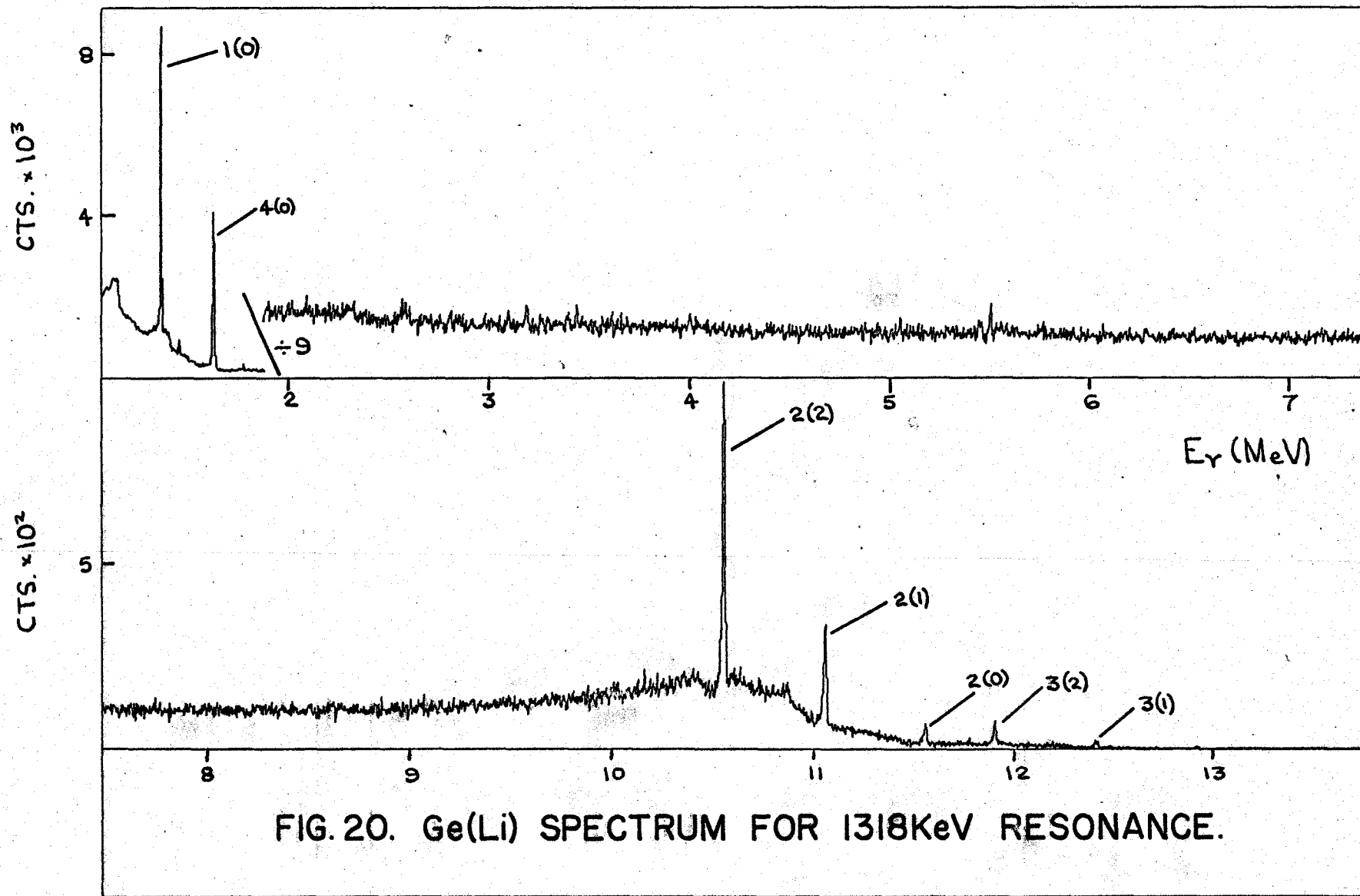


FIG. 20. Ge(Li) SPECTRUM FOR 1318KeV RESONANCE.

<u>Transition Number</u>	<u>Transition</u>
1	1.37 Mev $\rightarrow$ g.s.
2	Res. $\rightarrow$ 1.37 Mev
3	Res. $\rightarrow$ g.s.
4	$E_{\gamma} = 1.63$ Mev from Na <sup>23</sup> (p, $\alpha$ )Ne <sup>20</sup> reaction

TABLE 11: Identification of the peaks in the Ge(Li) Spectrum for the 1318 Kev Resonance.

used in the calculation. The Res.  $\rightarrow$  g.s. transition was not used in case any gamma rays were included from the same transition in the 1163 Kev resonance. It was found that for this resonance  $\Gamma_\gamma = 4.67 (\pm 1.12)$  ev. From this figure, and the branching ratios, the partial gamma widths for the transitions from the resonance were found and compared to Single Particle Estimates. These reduced widths are shown in Table 10.

(v)  $E_p = 1318$  Kev Resonance.

This resonance was studied with a NaOH target of around 5 Kev thickness at  $E_p \sim 1$  Mev. Gamma ray spectra were obtained at  $0^\circ$ ,  $55^\circ$ , and  $90^\circ$ . The  $55^\circ$  run is shown in Fig. 20, and the identification of the peaks is explained in Table 11. This represents a run of 2 hours duration at a proton current of around 2 microamps.

The decay scheme was found in the usual manner.

For the branching ratio work the normalization between runs was achieved using the readings from the "greater than 2 Mev" gate. The  $A_0$  value for the Res.  $\rightarrow$  1.37 transition was found from the angular distribution of the gamma rays concerned. This angular distribution was  $W(\theta) \propto 1 - 0.298 (\pm 0.3)P_2(\cos \theta) + 0.007 (\pm 0.25)P_4(\cos \theta)$ . Also for Ge(Li) efficiency curve work, the angular distribution of the 1.37 Mev  $\rightarrow$  g.s. was found. This angular distribution was  $W(\theta) \propto 1 - 0.155 (\pm 0.06)P_2(\cos \theta) + 0.08 (\pm 0.07)P_4(\cos \theta)$ . The  $A_0$

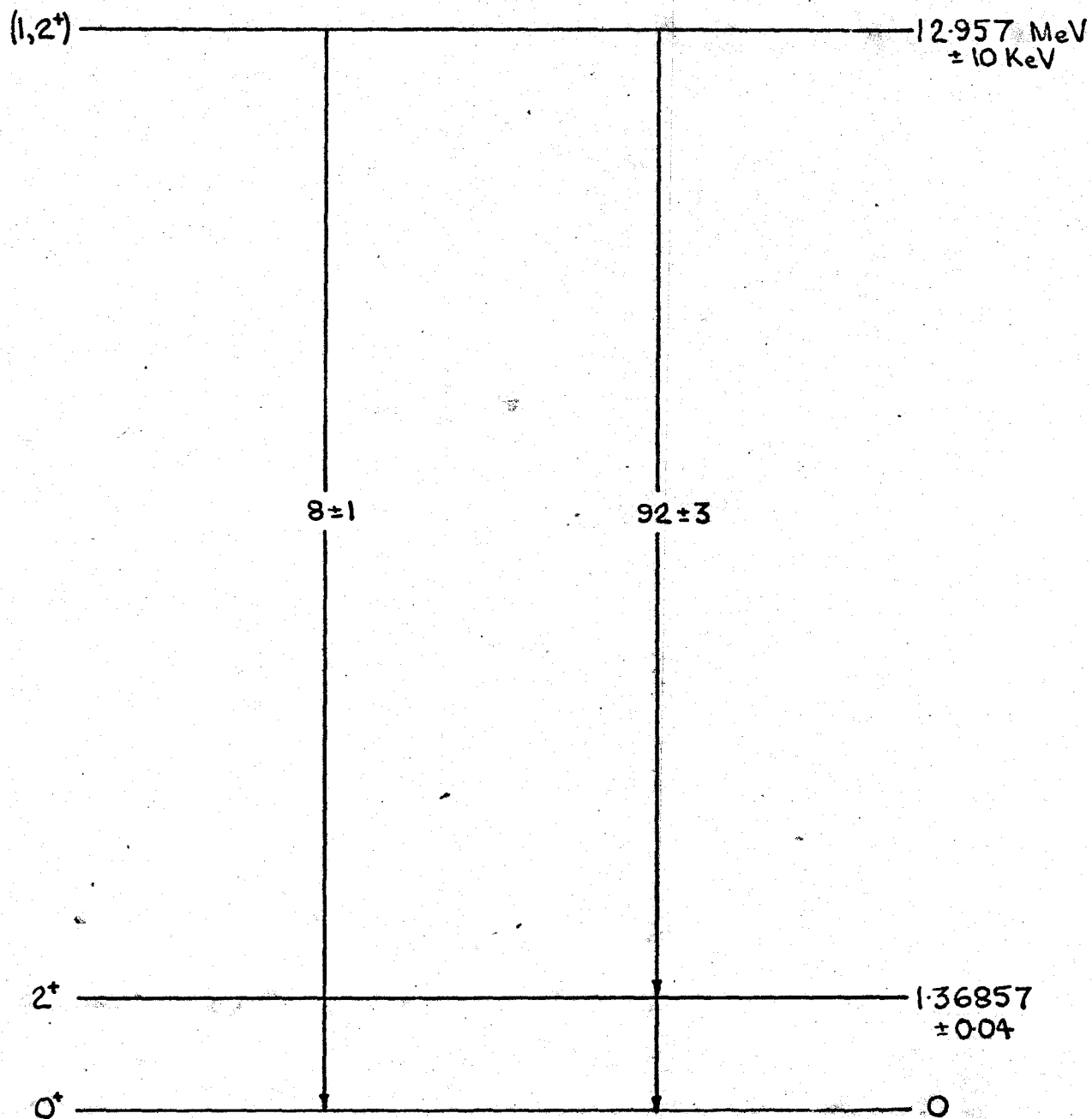
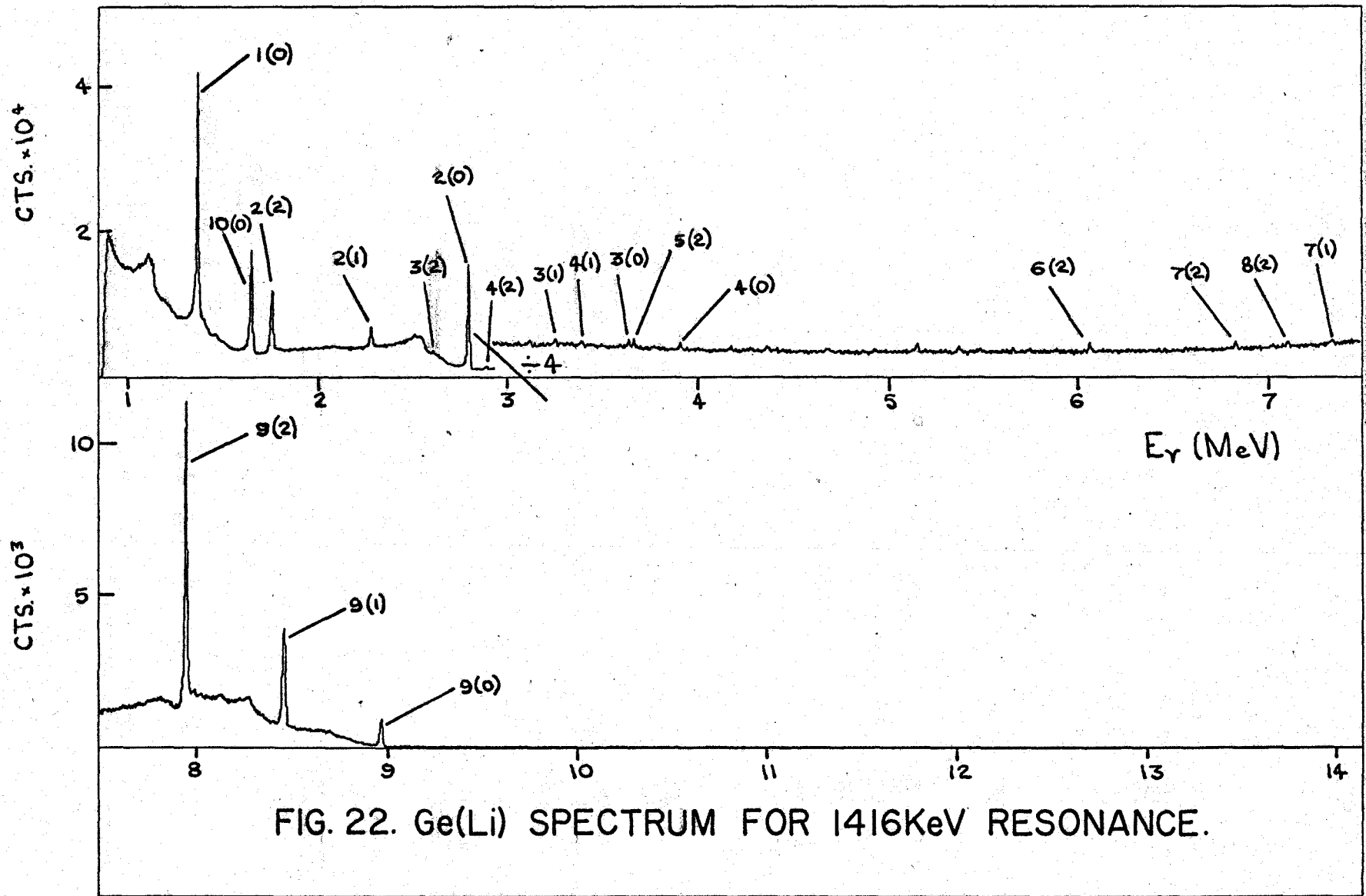


FIG. 21. DECAY SCHEME FOR 1318KeV RESONANCE.

<u>Transition</u>	$\frac{\Gamma_{\text{exp}}}{\Gamma(\text{E1})}$	$\frac{\Gamma_{\text{exp}}}{\Gamma(\text{M1})}$	$\frac{\Gamma_{\text{exp}}}{\Gamma(\text{E2})}$
<u>Spin 1</u>			
Res. $\rightarrow$ 1.37 Mev	$1.7 \times 10^{-2}$	$5 \times 10^{-1}$	$2 \times 10^1$
Res. $\rightarrow$ g.s.	$1.1 \times 10^{-3}$	$3.2 \times 10^{-2}$	
<u>Spin 2</u>			
R $\rightarrow$ 1.37 Mev		$3.1 \times 10^{-1}$	
R $\rightarrow$ g.s.			$6.4 \times 10^{-1}$

TABLE 12: Comparison to Single Particle Estimates for the 1318 Kev Resonance.



<u>Transition Number</u>	<u>Transition</u>
1	1.37 Mev $\rightarrow$ g.s.
2	4.12 Mev $\rightarrow$ 1.37 Mev
3	Res. $\rightarrow$ 9.46 Mev
4	5.23 Mev $\rightarrow$ 1.37 Mev
5	6.00 Mev $\rightarrow$ 1.37 Mev
6	Res. $\rightarrow$ 6.00 Mev
7	Res. $\rightarrow$ 5.23 Mev
8	9.46 Mev $\rightarrow$ 1.37 Mev
9	Res. $\rightarrow$ 4.12 Mev
10	$E_{\gamma} = 1.63$ Mev from Na <sup>23</sup> (p, $\alpha$ ) Ne <sup>20</sup> reaction

TABLE 13: Identification of the peaks in the Ge(Li) Spectrum for the 1416 Kev Resonance.

value for the Res.  $\rightarrow$  g.s. transition was found from the 55° run only.

The decay scheme, together with the branching ratios, is shown in Fig. 21. These figures agree almost exactly with those shown in Endt and Van der Leun (1967).

The gamma transition width for this resonance was found in an exactly similar way, and with the same target, as that used for the 1020 Kev resonance. It was found that for the 1318 Kev resonance  $\Gamma_\gamma = 17.1 (\pm 0.43)$  ev if spin 1 was used for the resonance, and  $\Gamma_\gamma = 10.3 (\pm 0.26)$  ev if spin 2 was used for the resonance. From these figures and from the branching ratios found, the partial gamma widths of the transitions from the resonance were found and compared to Single Particle Estimates. The reduced strengths are shown in Table 12. It can be seen that these reduced strengths in no way contradict the possible spin values of  $1^-$ ,  $1^+$  or  $2^+$  for the resonance.

(vi)  $E_p = 1416$  Kev Resonance.

This resonance was studied with a NaOH target of around 5 Kev thickness at  $E_p \sim 1$  Mev. Gamma ray spectra were measured on the Ge(Li) counter at 0°, 55°, and 90°. The 55° run is shown in Fig. 22 and the identification of the peaks is explained in Table 13. This represents a run of about 3 hours duration at a proton current of around 3 microamps.

The decay scheme was found in the usual manner.

For the branching ratio work the normalization between

runs were accomplished with the readings from the "greater than 2 Mev" gate. The  $A_0$  values for all the gamma rays in the Res.  $\rightarrow$  4.12 Mev  $\rightarrow$  1.37 Mev  $\rightarrow$  g.s. cascade were found from angular distributions of the gamma rays concerned.

The angular distributions found were as follows:-

<u>Transition</u>	<u>Angular Distribution</u>
Res. $\rightarrow$ 4.12 Mev	$W(\theta) \propto 1 + 0.478 (\pm 0.24)P_2(\cos \theta)$ $+ 0.15 (\pm 0.2)P_4(\cos \theta)$
4.12 Mev $\rightarrow$ 1.37 Mev	$W(\theta) \propto 1 + 0.406 (\pm 0.12)P_2(\cos \theta)$ $- 0.058 (\pm 0.15)P_4(\cos \theta)$
1.37 Mev $\rightarrow$ g.s.	$W(\theta) \propto 1 + 0.390 (\pm 0.04)P_2(\cos \theta)$ $- 0.057 (\pm 0.04)P_4(\cos \theta)$

The ratios of the  $A_0$  values found in this cascade were used in determining points on the Ge(Li) efficiency curve, as explained previously. The Res.  $\rightarrow$  4.12 Mev  $\rightarrow$  1.37 Mev cascade is known to be a 100% cascade and, originally, 95% of the 1.37 Mev  $\rightarrow$  g.s. transition was assumed to originate from the above cascade. This was based on figures from Endt and Van der Leun (1967). Fortunately, this 95% value turned out to be correct but the remaining 5% of the 1.37  $\rightarrow$  g.s. transition came from several other sources apart from the Res.  $\rightarrow$  1.37 Mev transition shown in Endt and Van der Leun.

The  $A_0$  values for all the other gamma transitions in the 1416 Kev resonance were found from the 55° run only.

The decay scheme, together with the branching ratios,

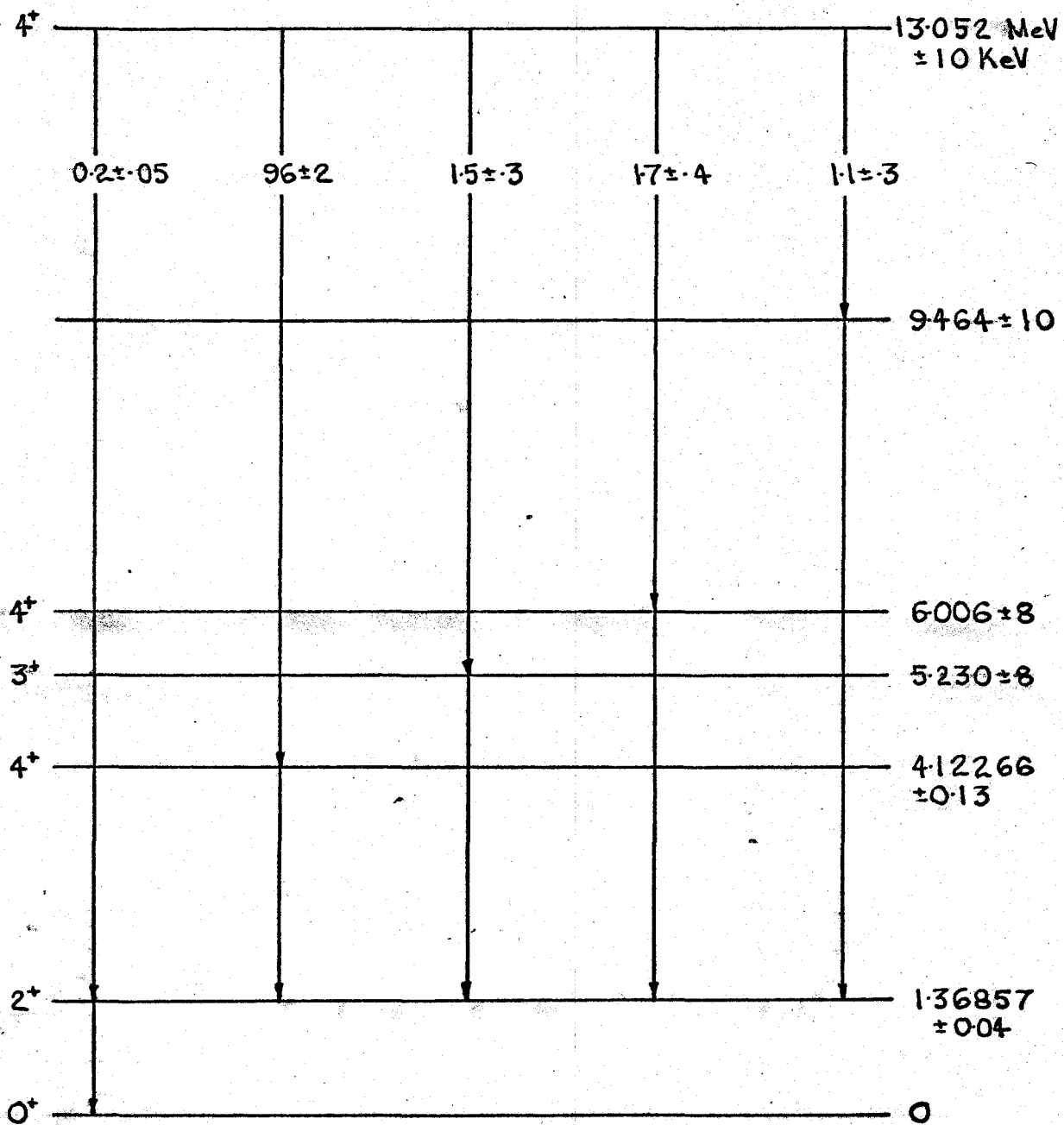


FIG.23. DECAY SCHEME FOR 1416KeV RESONANCE.

<u>Transition</u>	$\frac{\Gamma_{\text{exp}}}{\Gamma(\text{E1})}$	$\frac{\Gamma_{\text{exp}}}{\Gamma(\text{M1})}$	$\frac{\Gamma_{\text{exp}}}{\Gamma(\text{E2})}$	$\frac{\Gamma_{\text{exp}}}{\Gamma(\text{M2})}$
Res. → 4.12 Mev		$6.2 \times 10^{-1}$		
Res. → 9.46 Mev	$3.7 \times 10^{-2}$	$1.1 \times 10^{-1}$		$2 \times 10^3$
Res. → 5.23 Mev		$1.5 \times 10^{-2}$		
Res. → 6.00 Mev		$2.3 \times 10^{-2}$		
Res. → 1.37 Mev			$2.5 \times 10^{-2}$	

TABLE 14: Comparison to Single Particle Estimates for the 1416 Kev Resonance.

is shown in Fig. 23. It is interesting to note the inclusion of several energy levels hitherto unseen in NaI work, especially the 9.46 Mev level that has never been seen before in (p, $\gamma$ ) work on Na<sup>23</sup>.

The gamma transition width of this resonance was not found in the present series of experiments. However, the figure of  $\Gamma_\gamma = 9.3$  ev, given in Nordhagen, 1964, was used, together with the branching ratios found in the present experiment, to find the partial gamma widths of the transitions from the resonance. These partial gamma widths were compared to Single Particle Estimates and the reduced transition strengths are shown in Table 14.

Ollerhead, et al, (1968), have shown that the only possible spins for the 9.46 Mev level are  $2^-$ ,  $3^+$ , or  $4^-$ . From the reduced strengths shown in Table 14 it can be seen that a spin of  $2^-$  for the 9.46 Mev level is extremely unlikely, as this would mean that the Res.  $\rightarrow$  9.46 Mev is an M2 transition, with a reduced strength of  $2 \times 10^3$  Weisskopf Units, whereas no M2 transition is known in the s-d shell with a reduced strength of greater than a few Weisskopf Units (S.J. Skorka, 1966).

By studying the Doppler shift effect on a secondary in a cascade it is possible to arrive at some conclusions concerning the lifetime of the intermediate state. To illustrate this fact, it was found that the 9.46 Mev  $\rightarrow$

1.37 Mev transition, seen in the 1416 Kev resonance, exhibited essentially the full possible Doppler shift. It was, therefore, possible by considering the time taken for the  $\text{Mg}^{24}$  nucleus to slow down in the target material, to place an upper limit on the lifetime of the 9.46 Mev level of about  $10^{-13}$  secs, (Blaugrund, 1966). This, in turn, gave a level width of greater than  $6.6 \times 10^{-3}$  ev. Using this figure, and approximate branching ratios found from the work by Ollerhead et al (1968), the reduced strength of the 9.46 Mev  $\rightarrow$  1.37 Mev transition was found to be greater than 1.4 Weisskopf Units, if the spin of the 9.46 Mev level were  $4^-$ . In the above case the 9.46 Mev  $\rightarrow$  1.37 Mev transition would be an M2 transition, and, as has been previously stated, no M2 transition has been seen in the s-d shell with a reduced strength of greater than a Weisskopf Unit. Although the above argument does not entirely exclude the possibility of spin  $4^-$  for the 9.46 Mev level, the evidence for its exclusion is quite strong. Thus, the evidence tends to favour an assignment of  $3^+$  for the 9.46 Mev level.

### 3.3 Conclusion

From the studies reported in this thesis, several errors have been found in the decay schemes previously measured with NaI detectors. These errors involved either the reversal of the primary and secondary of a particular cascade, or the exclusion of weak transitions. The correction of

these errors was made possible due to the much increased resolution of Ge(Li) detectors over NaI detectors.

The branching ratio data found for the above decay schemes agreed quite well with that found from previous work.

In the reduced strength analysis the typical value for an M1 transition seems to be around  $10^{-1} \rightarrow 10^{-2}$  Weisskopf Units. This is a typical value for nuclei in this mass region, (Wilkinson, 1960). Very few E1 transitions were seen but the typical value of those that were observed was around  $10^{-3} \rightarrow 10^{-4}$  Weisskopf Units. These values are slightly weaker than those generally observed in this mass region.

From Doppler shift analysis a possible spin of  $3^+$  has been proposed for the 9.46 Mev level. Although no detailed work has as yet been done on this Doppler shift analysis, it is felt that this could prove a useful tool for assigning or limiting the spins of certain levels.

## BIBLIOGRAPHY

- Anderson, Dörum, Gautvik and Holtebekk, Nuclear Physics 22 (1961) 245.
- Blaugrund, Nuclear Physics 88 (1966) 501.
- Charlesworth, Private Communication (1967).
- Endt and Van der Leun, Energy Levels of  $Z = 11 - 21$  nuclei (IV), (North-Holland Publishing Company, Amsterdam, 1967).
- Enkelbertink and Endt, Nuclear Physics 88 (1966) 12-20.
- Feynman, Leighton and Sands, Lectures on Physics (Addison-Wesley Co. Inc., New York, 1963).
- Glaudemans and Endt, Nuclear Physics 30 (1962) 30.
- Gore, Nuclear Reactions, vol. 1 (North-Holland Publishing Company, Amsterdam, 1959).
- Mabey, M.Sc. Thesis, McMaster University (1968).
- Mourad, Nielsen and Petrilak, Nuclear Physics, A102 (1967) 406.
- Nordhagen and Steen, Physica Norvegica 1 (1964) 239.
- Ollerhead, Blackmore, Kuehner and Levesque. To be published in Canadian Journal of Physics (1968).
- Prosser, Unruh, Wildenthal and Krone, Physical Review 125 (1962) 594.
- Skorka, Compilation of Electromagnetic Transition Strengths, (Institut für Experimentalphysik der Universität, Hamburg, 1966).
- Whaling, Handbuch der Physik (Springer-Verlag, Berlin, 1958).
- Wilkinson, Nuclear Spectroscopy, ed. F. Ajzenberg-Selove, (New York: Academic Press, 1960).